Spectroscopic Investigations of Fragment Species in the Coma

Paul D. Feldman
The Johns Hopkins University

Anita L. Cochran
University of Texas

Michael R. Combi
University of Michigan

The content of the gaseous coma of a comet is dominated by fragment species produced by photolysis of the parent molecules issuing directly from the icy nucleus of the comet. Spectroscopy of these species provides complementary information on the physical state of the coma to that obtained from observations of the parent species. Extraction of physical parameters requires detailed molecular and atomic data together with reliable high-resolution spectra and absolute fluxes of the primary source of excitation, the Sun. The large database of observations, dating back more than a century, provides a means to assess the chemical and evolutionary diversity of comets.

1. INTRODUCTION

In 1964, P. Swings delivered the George Darwin lecture (*Swings,* 1965) on the one-hundredth anniversary of the first reported spectroscopic observation of a comet. He described a century of mainly photographic observations of what were recognized to be fragment species resulting from photochemical processes acting on the volatile species released from the cometary nucleus in response to solar heating. The features identified in the spectra were bands of the radicals OH, NH, CN, CH, C_3, C_2, and NH_2; the ions OH^+, CH^+, CO_2^+, CO^+, and N_2^+; Na I; and the forbidden red doublet of O I (*Swings and Haser,* 1956; *Arpigny,* 1965). By the time of the publication of the book *Comets* (*Wilkening,* 1982) 18 years later, optical spectroscopy had become quantitative photoelectric spectrophotometry (*A'Hearn,* 1982) and had been extended to the radio and vacuum ultraviolet (UV) (*Feldman,* 1982), yet the inventory of species detected grew slowly. In the visible, the Sun-grazing Comet Ikeya-Seki (C/1965 S1) showed the metals K, Ca^+, Ca, Fe, V, Cr, Mn, Ni, and Cu (*Preston,* 1967), presumably from the vaporization of refractory grains, and H_2O^+ was identified in Comet Kohoutek (C/1973 E1) a few years later. In the UV, the constituent atoms H, O, C, and S were detected together with CS and CO, the first "parent" molecule to be directly identified spectroscopically (*Feldman and Brune,* 1976).

The spectra of the observed radicals are necessarily complex and detailed analyses of high-resolution spectra demonstrated that the observed emission was produced for the most part by fluorescence of solar radiation. With this information, spectrophotometric data may be used to quantitatively derive column abundances of the observed species from which, with suitable modeling (see *Combi et al.,* 2004), the relative abundance of the parent species in the cometary ice could be deduced. Note that for some species, particularly C_2 and C_3, the identity of the parent still remains ambiguous. Long-slit spectroscopy at high spatial resolution has provided constraints on the photochemical parameters used in the models and also has served to probe physical conditions in the coma that produce deviations from the purely photochemical models. Similar analyses are also possible with narrowband photometric imaging (see *Schleicher and Farnham,* 2004).

Advances in infrared (IR) and radio technology, together with the timely apparitions of several active comets during the past 10 years, have led to the identification of more than two dozen parent volatile species in the coma (see *Bockelée-Morvan et al.,* 2004). During this same time enhancements in optical and UV technology have also permitted more detailed investigations of the spectra of (mainly) fragment species, leading to a more complete picture of the entire coma. The availability of state-of-the-art optical instrumentation at a given cometary apparition ensures the acquisition of datasets with good temporal coverage and comparability to the historical record for purposes of assessing diversity among comets. The high sensitivity of optical detectors also means that fragment species can be detected at larger heliocentric distances than any of the parents (cf. *Rauer et al.,* 2003). While notable advances have been made in spaceborne UV spectroscopic instrumentation, notably STIS on the Hubble

Space Telescope (HST) and the Far Ultraviolet Spectroscopic Explorer (FUSE) satellite, these resources are limited and cometary observations are relatively few.

2. PHYSICAL PROCESSES

2.1. Photolysis of Parent Molecules

The photolytic destruction of water, the dominant molecular species in the coma of comets at distances near 1 AU from the Sun, has been extensively studied (see *Combi et al.,* 2004). It may proceed through multiple paths depending on the energy of the incident solar photon (here given as the threshold wavelength):

$H_2O + h\nu \rightarrow$	$OH + H$	2424.6 Å
$\rightarrow$	$OH(A^2\Sigma^+) + H$	1357.1 Å
$\rightarrow$	$H_2 + O(^1D)$	1770 Å
$\rightarrow$	$H_2 + O(^1S)$	1450 Å
$\rightarrow$	$H + H + O(^3P)$	1304 Å
$\rightarrow$	$H_2O^+ + e$	984 Å
$\rightarrow$	$H + OH^+ + e$	684.4 Å
$\rightarrow$	$H_2 + O^+ + e$	664.4 Å
$\rightarrow$	$OH + H^+ + e$	662.3 Å

Many of the fragments can be further broken down:

$OH + h\nu \rightarrow$	$O + H$	2823.0 Å
$\rightarrow$	$OH^+ + e$	928 Å
$H_2 + h\nu \rightarrow$	$H + H$	844.79 Å
$\rightarrow$	$H_2^+ + e$	803.67 Å
$\rightarrow$	$H + H^+ + e$	685.8 Å
$O + h\nu \rightarrow$	$O^+ + e$	910.44 Å
$H + h\nu \rightarrow$	$H^+ + e$	911.75 Å

The last two reactions may also occur by resonant charge exchange with solar wind protons. Photoelectrons produced in the ionization process, particularly those from the strong solar He II line at 304 Å, also lead to secondary dissociation and ionization (*Cravens et al.,* 1987) and may contribute to the observed emissions.

Similar equations may be written for other cometary species and many, particularly some of the more abundant ones such as CO and CO_2, produce many of the same fragment species. *Huebner et al.* (1992) have compiled a very useful list of photodestruction rates for a large number of molecules that includes many polyatomic species that have been identified as being present in the cometary ice (see Table 1 of *Bockelée-Morvan et al.,* 2004).

For the case of H_2O, all the fragment species listed above, with the exception of H^+ and H_2^+, have been detected spectroscopically. The second through fourth reactions listed above leave the product atom or molecule in an excited state that leads to "prompt" emission of a photon. This provides a means for mapping the spatial distribution of the parent molecule in the inner coma. Prompt emission includes both allowed radiative decays (such as from the $A^2\Sigma^+$ state of OH) as well as those from metastable states such as $O(^1D)$, whose lifetime is ~130 s. The O I ^1D–^3P doublet at 6300 and 6364 Å has been used extensively as a ground-based surrogate for the determination of the water production rate with the caveat that other species such as OH, CO, and CO_2 may also populate the upper level. When the density of H_2O is sufficient to produce observable 6300 Å emission, it may also produce collisional quenching of the ^1D state, and this must be included in the analysis. The analogous ^1D–^3P transitions in C occur at 9823 and 9849 Å and can similarly give information about the production rate of CO. Carbon atoms in the ^1D state, whose lifetime is ~4000 s, are known to be present from the observation of the resonantly scattered $^1P^o$–^1D transition at 1931 Å (*Tozzi et al.,* 1998). To date the IR lines have only been detected in Comets 1P/Halley and Hale-Bopp (C/1995 O1) (*Oliversen et al.,* 2002).

2.2. Excitation Mechanisms

The extraction of coma abundances from spectrophotometric measurements of either the total flux or the surface brightness in a given spectral feature has been summarized by *Feldman* (1996) and we repeat some of the salient points here. We note that the uncertainty in the derived abundances may include not only the measurement uncertainty, but also uncertainties in the atomic and molecular data and, in the case of surface brightness measurements, uncertainties in the model parameters used. One must be careful in comparing abundances and production rates derived by different observers for the same comet at a given time to assure that comparable physical and model parameters are used.

In the simplest case we begin with the total number of species i in the coma

$$M_i = Q_i \tau_i(r) \quad (1)$$

where Q_i is the production rate (atoms or molecules s^{-1}) of all sources of species i and $\tau_i(r)$ is the lifetime of this species at heliocentric distance r, $\tau_i(r) = \tau_i(1\ \mathrm{AU})r^2$.

For an optically thin coma, the luminosity, in photons $cm^{-2}\ s^{-1}$, in a given atomic or molecular transition at wavelength λ, is

$$L(\lambda) = M_i g(\lambda,r) \quad (2)$$

where the fluorescence efficiency, or "g-factor", $g(\lambda,r) = g(\lambda,1\ \mathrm{AU})r^{-2}$, is defined by *Chamberlain and Hunten* (1987) in cgs units as

$$g(\lambda,1\ \mathrm{AU}) = \frac{\pi e^2}{mc^2}\lambda^2 f_\lambda \pi F_\odot \tilde{\omega}\ \text{photons}\ s^{-1}\ \text{atom}^{-1} \quad (3)$$

Here, e, m, and c have their usual atomic values; λ is the transition wavelength; f_λ is the absorption oscillator strength;

$\pi F_\odot$ is the solar flux per unit wavelength interval at 1 AU; and $\tilde{\omega}$ is the albedo for single scattering, defined for a line in an atomic multiplet as

$$\tilde{\omega} = \frac{A_j}{\Sigma_j A_j} \quad (4)$$

and A_j is the Einstein transition probability. At low and moderate spectral resolution, a given multiplet is not resolved and in this case $\tilde{\omega} = 1$. For diatomic molecules, fluorescence to other vibrational levels becomes important and the evaluation of $\tilde{\omega}$ depends to a large degree on the physical conditions in the coma. Note that this definition differs from equation (3) of *Bockelée-Morvan et al.* (2004) in that a blackbody cannot be used to represent the solar flux, particularly in the UV, and that a high-resolution spectral atlas is required to account for the Fraunhofer structure in the solar spectrum.

Then, for a comet at a geocentric distance Δ, the total flux from the coma at wavelength λ is

$$F(\lambda) = \frac{L(\lambda)}{4\pi\Delta^2} = \frac{Q_i g(\lambda,r)\tau_i(r)}{4\pi\Delta^2} \text{ photons cm}^{-2}\text{ s}^{-1} \quad (5)$$

Note that the product $g(\lambda,r)\tau_i(r)$ is independent of r.

Unfortunately, the scale lengths (the product of lifetime and outflow velocity) of almost all the species of interest in the UV are on the order of 10^5–10^6 km at 1 AU. Thus, total flux measurements require fields of view ranging from several arcminutes to a few degrees. This has been done only rarely (*Woods et al.,* 2000). Again assuming an optically thin coma, the measured flux in the aperture, $F'(\lambda)$, can be converted to an average surface brightness (in units of rayleighs), $B(\lambda)$

$$B(\lambda) = 4\pi 10^{-6} F'(\lambda)\Omega^{-1} \quad (6)$$

where Ω is the solid angle subtended by the aperture. The brightness, in turn, is related to $\bar{N}_i$, the average column density of species i within the field of view by

$$B(\lambda) = 10^{-6} g(\lambda,r)\bar{N}_i \quad (7)$$

At this point the evaluation of Q_i from $\bar{N}_i$ requires the use of a model of the density distribution of the species i (see *Combi et al.,* 2004).

2.2.1. Fluorescence equilibrium. The excitation of the electronic transitions of the radicals observed in the visible and near-UV, which may have many photon absorption and emission cycles in their lifetime, leads to "fluorescence equilibrium" of the rotational levels within the ground vibrational level. This process and the various factors that affect it are fully discussed in section 3.1.4 of *Bockelée-Morvan et al.* (2004). In contrast, in the far-UV, where the solar flux is low, it is often the case that the probability of absorption of a solar photon is less than the probability that the species will be dissociated or ionized, so that the ground state population is not affected by fluorescence and can be described by a Boltzmann distribution at a suitable temperature corresponding to the cometary environment where the species was produced. For prompt emission, such as that from CO produced by photodissociative excitation of CO_2 (*Mumma et al.,* 1975), the rotational temperature of the CO will be ~5 times larger than the rotational temperature of the CO_2 because of the factor of 5 in the rotational constants and the need to conserve angular momentum in the dissociation process. Similarly, prompt emission of OH will also be characterized by a "hot" rotational distribution (*Bertaux,* 1986; *Budzien and Feldman,* 1991).

2.2.2. Swings and Greenstein effects. *Swings* (1941) pointed out that because of the Fraunhofer absorption lines in the visible region of the solar spectrum, the absorption of solar photons in a given molecular band would vary with the comet's heliocentric velocity, $\dot{r}$, leading to differences in the structure of a band at different values of $\dot{r}$ when observed at high spectral resolution. This effect is now commonly referred to as the Swings effect. Even for observations at low resolution, the Swings effect must be taken into account in the calculation of total band g-factor, and this has been done for a number of important species such as OH, CN, and NH. A particularly important case is that of the OH $A^2\Sigma^+$–$X^2\Pi$ (0,0) band at ~3085 Å, which is often used to derive the water production rate (*Scheicher and A'Hearn,* 1988).

While this effect was first recognized in the spectra of radicals in the visible, a similar phenomenon occurs in the excitation of atomic multiplets below 2000 Å, where the solar spectrum makes a transition to an emission line spectrum. For example, the three lines of O I λ1302 have widths of ~0.1 Å, corresponding to a velocity of ~25 km s^{-1}, so that knowledge of exact solar line shapes is essential to a reliable evaluation of the g-factor for this transition (*Feldman et al.,* 1976; *Feldman,* 1982).

A differential Swings effect occurs in the coma since atoms and molecules on the sunward side of the coma, flowing outward toward the Sun, have a net velocity that is different from those on the tailward side, and so if the absorption of solar photons takes place on the edge of an absorption (or emission) line, the g-factors will be different in the sunward and tailward directions. Differences of this type will appear in long-slit spectra in which the slit is placed along the Sun-comet line. This effect was pointed out by *Greenstein* (1958). An analog in the far-UV has been observed in the case of O I λ1302. The measurement of a Greenstein effect in OH in Comet 2P/Encke has been used to derive the outflow velocity of water and consequently the nongravitational acceleration of the comet (*A'Hearn and Schleicher,* 1988).

2.2.3. Bowen fluorescence. As noted above, in the UV, with the exception of the H I Lyman series, solar line widths are such that for comets with heliocentric velocities

>25 km s^{-1}, the available flux at the center of the absorbing atom's line is reduced to a very small value. It was thus surprising that the O I λ1302 line appeared fairly strongly in the observed spectrum of Comets Kohoutek (C/1973 E1) and West (C/1975 V1), whose values of $\dot{r}$ were both >45 km s^{-1} at the times of observation. The explanation invoked the accidental coincidence of the solar H I Lyman-β line at 1025.72 Å with the O I ^3D–^3P transition at 1025.76 Å, cascading through the intermediate ^3P state (*Feldman et al.,* 1976). This mechanism, well known in the study of planetary nebulae, is referred to as Bowen fluorescence (*Bowen,* 1947). The g-factor due to Lyman-β pumping is an order of magnitude smaller than that for resonance scattering, but sufficient to explain the observations. Lyman-β is also coincident with the P1 line of the (6,0) band of the H_2 Lyman system ($B^1\Sigma^+$–$X^1\Sigma_g^+$), leading to fluorescence in the same line of several (6,v") bands. Three such lines have recently been detected in the FUSE spectra of Comet C/2001 A2 (LINEAR) (*Feldman et al.,* 2002).

It is interesting to note that fluorescence excited by solar H I Lyman-α was considered by *Haser and Swings* (1957) but considered unlikely based on the state of spectroscopic knowledge at that time. Lyman-α fluorescence of CO in the Fourth Positive system was first detected in the spectrum of Venus (*Durrance,* 1981) and observed in 1996 in Comet Hyakutake (C/1996 B2) (*Wolven and Feldman,* 1998).

2.2.4. Electron impact excitation. We noted above that photoelectron impact excitation may also contribute to the observed emissions, particularly in the UV. However, a very simple argument, based on the known energy distribution of solar UV photons, demonstrates that this is only a minor source for the principal emissions. Since the photoionization rate of water (and of the important minor species such as CO and CO_2) is on the order of 10^{-6} s^{-1} at 1 AU, and the efficiency for converting the excess electron energy into excitation of a single emission is on the order of a few percent, the effective excitation rate for any emission will be on the order of 10^{-8} s^{-1} or less at 1 AU (*Cravens and Green,* 1978). Since the efficiencies for resonance scattering or fluorescence for almost all the known cometary emissions are one to several orders of magnitude larger, electron impact may be safely neglected except in a few specific cases. These are the forbidden transitions, where the oscillator strength (and consequently the g-factor) is very small. Examples include the O I $^5S_2$–$^3P_{2,1}$ doublet at 1356 Å, the O I ^1D–^3P red lines at 6300 and 6364 Å, observed in many comets, and the CO Cameron bands (*Weaver et al.,* 1994; *Feldman et al.,* 1997). However, the excitation of these latter two is dominated by prompt emission in the inner coma. Some of the emissions below 1200 Å observed in the FUSE spectrum of Comet C/2001 A2 (LINEAR) have also been attributed to electron impact (*Feldman et al.,* 2002).

2.2.5. Solar cycle variation. The relative abundance of a fragment species depends on the absorption cross section (σ_d) and the solar flux seen by the comet. The rate coefficient J_d is evaluated at 1 AU using whole-disk measurements of the solar flux by integrating the cross section

$$J_d = \int_0^{\lambda_{th}} \pi F_\odot \sigma_d \, d\lambda \qquad (8)$$

These rates may also be estimated from the threshold energies shown in the table of reactions given in section 2.1, since the solar flux is decreasing very rapidly to shorter wavelengths. Processes with thresholds near 3000 Å have lifetimes on the order of 10^4 s, those with thresholds near 2000 Å an order of magnitude longer, while those with thresholds below Lyman-α, such as most photoionization channels, have lifetimes on the order of 10^6 s, all at 1 AU. In addition to uncertainties in the details of the absorption cross sections, further uncertainty is introduced into the calculation of J_d by the lack of exact knowledge of the solar flux at the time of a given observation due to the variability of the solar radiation below 2000 Å, and most importantly, below Lyman-α. The solar UV flux is known to vary considerably both with the 27-d solar rotation period and with the 11-yr solar activity cycle, the latter reaching factors of 2 to 4 for wavelengths shortward of 1000 Å (*Lean,* 1991). Also, at any given point in its orbit, a comet may see a different hemisphere of the Sun than what is seen from Earth. The compilation of photodestruction rates of *Huebner et al.* (1992) uses mean solar fluxes to represent the extreme conditions of solar minimum and solar maximum and also includes the evaluation of the excess energies of the dissociation products.

3. SPECTROSCOPIC OBSERVATIONS

3.1. Ultraviolet Observatories in Space

The first observations of comets in the spectral region below 3000 Å were made from space in 1970 by the Orbiting Astronomical Observatory (OAO-2). The spectrum of Comet Bennett (C/1969 Y1) showed very strong OH emission at ~3085 Å and H I Lyman-α emission, at 1216 Å, principal dissociation products of H_2O (*Code et al.,* 1972). *Feldman* (1982) reviewed satellite and sounding rocket observations made before the launch of the International Ultraviolet Explorer (IUE) satellite observatory in 1978 and the early results from IUE, which observed more than 50 comets before it was shut down in September 1996 [see *Festou and Feldman* (1987) for a review of the principal results through 1986].

The HST, launched in 1990, made a significant advance in UV sensitivity and provided the ability to observe in a small field of view very close to the nucleus. Two spectrographs, the Goddard High Resolution Spectrograph (GHRS), which utilized solar blind detectors exclusively for UV spectroscopy, and the Faint Object Spectrograph (FOS), were used extensively through 1997 (*Weaver,* 1998). In February of that year they were replaced by the Space Telescope Imaging Spectrograph (STIS), which provided further enhancements including long-slit spectroscopy with an angular

TABLE 1. Principal optical spectroscopic features of cometary fragment species.

Species*	Transition	System Name	Wavelength (Å)
OH	$A^2\Sigma^+$–$X^2\Pi_i$ (0,0)		3085
CN	$B^2\Sigma^+$–$X^2\Sigma^+$ (0,0)	Violet	3883
	$A^2\Pi$–$X^2\Sigma^+$ (2,0)	Red	7873
C_2	$d^3\Pi_g$–$a^3\Pi_u$ (0,0)	Swan	5165
	$A^1\Pi_u$–$X^1\Sigma_g^+$ (3,0)	Phillips	7715
	$D^1\Sigma_u^+$–$X^1\Sigma_g^+$ (0,0)	Mulliken	2313
C_3	$\tilde{A}^1\Pi_u$–$\tilde{X}^1\Sigma_g^+$	Comet Head Group	3440–4100
CH	$A^2\Delta$–$X^2\Pi$ (0,0)		4314
	$B^2\Sigma^-$–$X^2\Pi$ (0,0)		3871, 3889
CS	$A^1\Pi$–$X^1\Sigma^+$ (0,0)		2576
NH	$A^3\Pi_i$–$X^3\Sigma^-$ (0,0)		3360
NH_2	$\tilde{A}^2A_1$–$\tilde{X}^2B_1$		4500–7350
O I ^1D	^1D–^3P		6300, 6364
O I ^1S	^1S–^1D		5577
C I ^1D	^1D–^3P		9823, 9849
CO^+	$B^2\Sigma^+$–$X^2\Sigma^+$ (0,0)	First Negative	2190
	$A^2\Pi$–$X^2\Sigma^+$ (2,0)	Comet Tail	4273
CO_2^+	$\tilde{B}^2\Sigma_u$–$\tilde{X}^2\Pi_g$		2883, 2896
	$\tilde{A}^2\Pi_u$–$\tilde{X}^2\Pi_g$	Fox-Duffendack-Barker	2800–5000
CH^+	$A^1\Pi$–$X^1\Sigma^+$ (0,0)	Douglas-Herzberg	4225, 4237
OH^+	$A^3\Pi$–$X^3\Sigma^-$ (0,0)		3565
H_2O^+	$\tilde{A}^2A_1$–$\tilde{X}^2B_1$		4270–7540
N_2^+	$B^2\Sigma^+$–$X^2\Sigma^+$ (0,0)	First Negative	3914

*CO is both a dissociation product and a native molecular species and is discussed by *Bockelée-Morvan et al.* (2004).

resolution of 50 milliarcsec. Except for some early results on Comet Hale-Bopp (C/1995 O1) (*Weaver et al.,* 1999), the spectroscopic results from STIS observations of several comets remain to be published, although a few will be described below. Finally, we note the launch in 1999 of FUSE, which provides access to the spectral region between 900 and 1200 Å at very high spectral resolution (*Feldman et al.,* 2002; *Weaver et al.,* 2002).

3.2. Optical Capabilities

As mentioned in the introduction, the spectrum of a comet was first observed in 1864. From then until the 1970s, optical cometary spectra were primarily obtained using photographic plates. At that point, observations began to switch over to photoelectric detectors of various types; optical cometary spectra are obtained currently almost exclusively using CCD detectors.

The optical spectrum of comets is quite dense because it consists mostly of molecular bands. The principal spectral features are listed in Table 1. Optical spectra are generally obtained in one of two spectral resolution regimes: moderate resolving powers of $R = \lambda/\Delta\lambda \sim 600$, which allow detection of complete bands but not individual lines, or $R >$ 10,000, which allow detection of individual lines. The majority of extant cometary spectra were obtained in the moderate-resolution mode, an example of which is shown in Fig. 1, with fewer than 25 comets observed at high spectral resolving powers. The choice of the spectral bandpass is generally dependent on the detector. Some groundbased spectrographs are capable of being used at ~3085 Å to observe the OH (0,0) band, but low detector quantum efficiency and poor atmospheric throughput make such observations difficult.

Typically, slit widths of 2–4 arcsec on the sky are used when obtaining cometary spectra, with the spectral resolution defined in part by this width. One exception is observations obtained with an imaging Fabry-Pérot spectrograph where the resolution is obtained by tuning the etalons (cf. *Magee-Sauer et al.,* 1988) and a large region of the sky can be imaged onto the detector. Fabry-Pérot instruments generally have a very limited bandpass but work at relatively high spectral resolving powers.

Since comets are spatially large, it is desirable to obtain spectra at different positions in the coma. Generally, this is done either by use of a "long" slit (generally 30–150 arcsec) or by repositioning the telescope to image different regions of the coma or both. In order to sample all directions in the coma with a long slit instrument, the slit must be rotated to different position angles on the sky and additional observations obtained. Alternatively, a fiber-fed spectrograph can

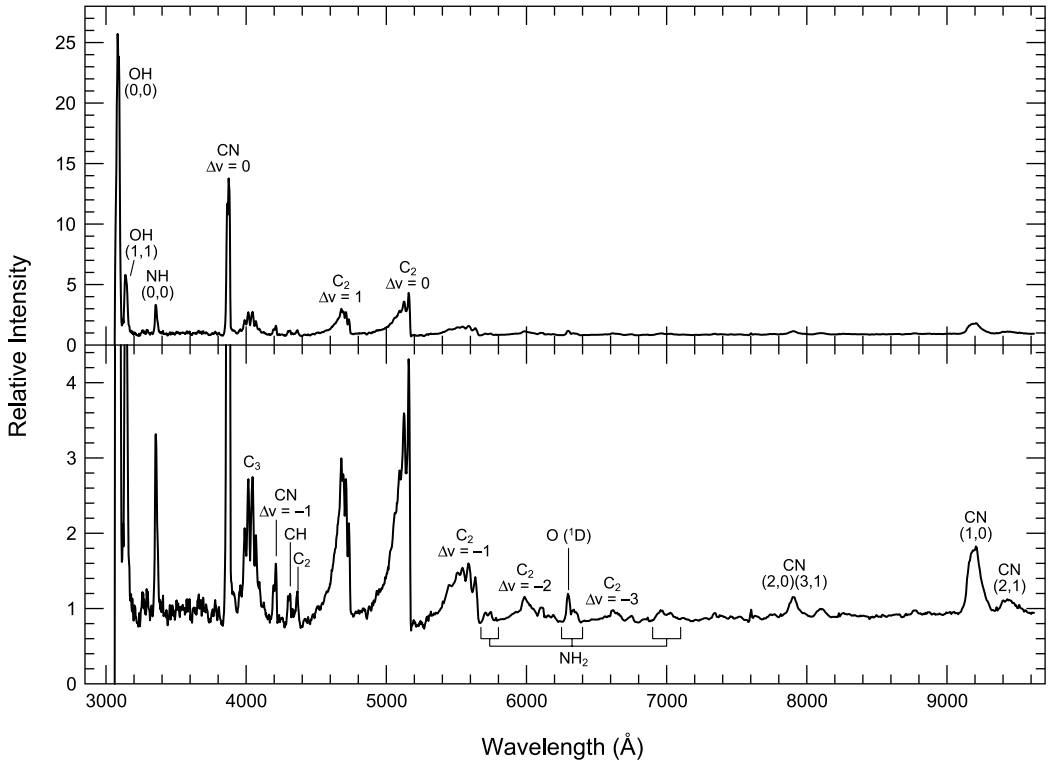

Fig. 1. Optical/near-IR CCD spectrum of Comet 109P/Swift-Tuttle obtained November 26, 1992. This spectrum is a composite of a UV/blue spectrum of Cochran (personal communication) and a red/near-IR spectrum of *Fink and Hicks* (1996). The cometary spectrum has been divided by a solar spectrum to show the cometary emissions. The two-pixel resolution was ~7 Å for the blue and ~14 Å for the red half. The upper panel shows the spectrum scaled by the strongest feature while the lower panel has an expanded ordinate to show the weaker features. The main features are labeled in one of the panels. This spectrum is typical of comets in the inner solar system.

use fibers placed throughout the coma to obtain spatial information. The fiber pattern can be linear or can sample in many directions simultaneously.

In addition to spectra, cometary comae may be studied using narrow-band photometry or wide-field imaging (see *Schleicher and Farnham,* 2004). Narrow-band photometry allows for observations of fainter comets and the outer regions of the comae; spectra allow for discrimination between crowded spectral features but suffer from small apertures resulting in longer integration times.

3.3. Infrared

Rapid advances in near-IR (~1–5 μm) spectroscopic instrumentation, particularly at the Keck Telescopes and the Infrared Telescope Facility at Mauna Kea, have led to much new information about the molecular composition of the inner coma. Representative spectra given by *Mumma et al.* (2001) disclose the presence of a wide variety of cometary organic molecules, discussed in detail in *Bockelée-Morvan et al.* (2004). The exception is OH, which appears mainly in transitions from highly excited rotational levels, implying that the excitation source is prompt emission following the dissociation of water.

3.4. Radio

Fluorescence pumping through the UV transitions of the OH radical produces a deviation of the population of the hyperfine and Λ-doublet levels of the $X^2\Pi_{3/2}$ (J = 3/2) ground state from statistical equilibrium (*Despois et al.,* 1981; *Schleicher and A'Hearn,* 1988). Depending on the heliocentric velocity, this departure may be either "inverted" or "anti-inverted," giving rise to either stimulated emission or absorption against the galactic background at 18 cm wavelength. This technique has been used extensively since 1973 to monitor the OH production rate in comets (*Crovisier et al.,* 2002). The resulting radio emissions are easily quenched by collisions with molecules and ions, the latter giving rise to a fairly large "collision radius" that must be accounted for in interpreting the derived OH column density.

4. WATER PRODUCTS

4.1. Hydroxyl Radical

The OH radical is the easiest dissociation product of water to observe, and is often used to determine the production rate of water and to serve as a standard to which

all other coma abundances are compared. Fortunately, there are three separate largely self-consistent datasets that provide measurements of OH in a large number of comets made during the past 20 years or more. However, the determination of water production rate from the data differs for the three and the derived rates are often not in agreement. The first is the set of groundbased photometric measurements at ~3085 Å made through standardized narrow-band filters, exemplified by the work of *A'Hearn et al.* (1995). These measurements are discussed in *Schleicher and Farnham* (2004). The second is the set of observations of the 18-cm radio lines of OH in more than 50 comets made at the Nançay radio telescope dating back to 1973 (*Crovisier et al.,* 2002). The third set, also comprising over 50 cometary apparitions between 1978 and 1996, is the spectroscopic measurement of OH fluorescence at ~3085 Å from the orbiting IUE. This satellite was in geosynchronous Earth orbit and its optical performance, which was monitored continuously, did not degrade significantly with time, ensuring a reliable calibration of all the observations. There are also many other spectroscopic observations of OH in both the radio and the UV, the latter from both HST and from high-altitude groundbased observatories.

Interpretation and intercomparison of the radio and UV observations are dependent on an accurate knowledge of the UV pumping of the inversion of the Λ-doubled ground state of the molecule, as described above in section 3.4. The two measurements are fundamentally different and so the comparison relies on extensive modeling, both of the spatial distribution and outflow velocity of the OH radicals in the coma, and of the solar excitation process. With high spectral resolution in the UV, the individual ro-vibrational lines of the band can be resolved and such measurements serve as a validation of the fluorescence calculation, which depends in turn on a high-resolution spectrum of the Sun (*Scheicher and A'Hearn,* 1988). But this resolution cannot match that available with the 18-cm radio lines, which in velocity space can reach ~0.3 km s^{-1}, thus permitting the determination of the kinematic properties of the outflowing gas (*Bockelée-Morvan and Gérard,* 1984; *Bockelée-Morvan et al.,* 1990; *Tacconi-Garman et al.,* 1990). *Bockelée-Morvan et al.* (1990) demonstrated variations in OH velocity with both cometocentric and heliocentric distance from an extensive set of observations of Comet 1P/Halley. Collisional quenching of the ground state inversion affects the radio lines but not the UV, but the strongest UV lines can saturate at OH column densities that are reached near the nucleus, and small field-of-view observation from HST show indications of this effect. With their models constrained by the velocity measurements, *Bockelée-Morvan et al.* (1990) and *Gérard* (1990) were able to reconcile the water production rates derived from the 18-cm observations with those derived from IUE observations of Comet 1P/Halley over an extended range of heliocentric distance. Modeling by *Combi and Feldman* (1993) was able to achieve agreement between the production rates for Comet 1P/Halley derived from the OH UV data and those derived from H I Lyman-α, both observed nearly simultaneously by IUE. A similar result was obtained for Comet 21P/Giacobini-Zinner (*Combi and Feldman,* 1992).

Bockelée-Morvan and Gérard (1984) also noted asymmetries in both the velocity structure and the spatial distribution of the 18-cm lines in three comets, which they attributed to asymmetrical outgassing of the nucleus. A similar result was reported by *A'Hearn and Schleicher* (1988) using the Greenstein effect to demonstrate asymmetrical outgassing of the nucleus of Comet 2P/Encke.

OH has also been detected in high-resolution IR spectra near 3 μm of several recent comets (*Brooke et al.,* 1996; *Mumma et al.,* 2001). From the spatial profiles of individual lines, *Brooke et al.* (1996) demonstrated that the lines originating from high rotational levels follow that of the parent molecule, H_2O, and therefore that these lines arise from prompt emission, while the lower excitation lines were flatter and the result of UV fluorescence. These observations have not yet been quantitatively exploited for the determination of production rates. The OH $A^2\Sigma^+$–$X^2\Pi$ (0,0) band at ~3085 Å also exhibits a "hot" rotational distribution near the nucleus due to prompt emission (*Bertaux,* 1986). Detection of this prompt emission, which dominates fluorescence only at distances of less than 100 km from the nucleus, requires high spatial resolution, which was afforded the IUE by the close approach of Comet IRAS-Araki-Alcock (C/1983 H1) to Earth in 1983 (*Budzien and Feldman,* 1991).

Finally, we note that the UV (0,0) band, in fluorescence equilibrium, consists of a small number of individual lines that are well separated at a spectral resolution of ≤1 Å. This led *A'Hearn et al.* (1985) to calculate the analogous spectrum of OD. While they found that the strongest lines of OD are separable from the OH lines, and are particularly enhanced at heliocentric velocities between –30 and –5 km s^{-1}, attempts to date to detect these lines with both IUE and HST have not been successful.

4.2. Atomic Hydrogen

Following the first observation of the large H I Lyman-α coma surrounding Comet Bennett (C/1969 Y1) in 1970 by two Earth-orbiting spacecraft (*Code et al.,* 1972; *Bertaux et al.,* 1973), this emission has been observed in a large number of comets both with imaging detectors and spectrographs on a variety of sounding rockets, orbiting observatories, and various other spacecraft. Initial modeling of the spatial distribution, taking into account the excess velocities of multiple sources, solar radiation pressure, and radiative transfer effects, was summarized by *Keller* (1976). A more complete discussion of the physics involved in the photochemical production of H atoms and their subsequent non-LTE (local thermodynamic equilibrium) collisional coupling to the coma is given in *Combi et al.* (2004). In this section we will limit the discussion to spectroscopic observations made at sufficient resolution to allow the determination of the velocity distribution of the H atoms and the presence of radiation trapping near the nucleus, which are relatively few

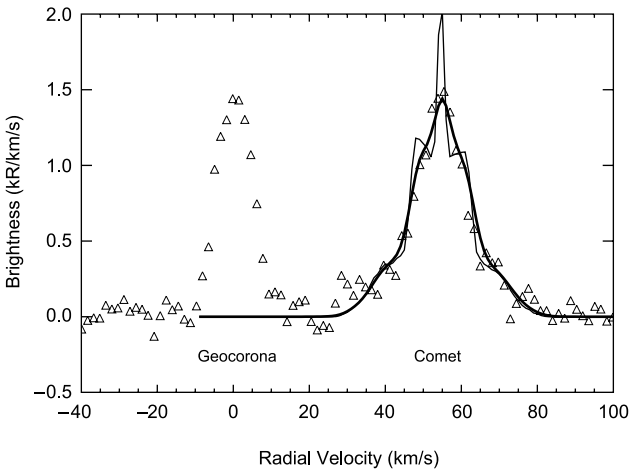

Fig. 2. Hydrogen Lyman-α line profile in Comet C/1996 B2 (Hyakutake). The triangles show the observed line profile obtained with the GHRS instrument on HST with the small science aperture located at a point 111,000 km sunward of the position of the nucleus, which is in the optically thin region of the coma. The thin line shows the intrinsic emission from the comet at very high spectral resolution (1 km s^{-1}) as calculated by the model of *Combi et al.* (1998). The thicker line is the model convolved with the instrument spectral function (4 km s^{-1} resolution). The emission of H in the geocorona is the line at 0 km s^{-1} to the left of the comet line, and the comet's emission is Doppler shifted to the comet's 55 km s^{-1} relative geocentric velocity (from *Combi et al.,* 1998).

(*Festou et al.,* 1979; *Combi et al.,* 1998). Very high spectral resolution has also been obtained using Fabry-Pérot interferometry and coudé/echelle spectroscopy to observe the Hα line at 6563 Å (*Huppler et al.,* 1975; *Scherb,* 1981; *Brown and Spinrad,* 1993; *Combi et al.,* 1999).

Combi et al. (1998) showed Lyman-α line profiles measured with the GHRS on HST obtained with a spectral sampling of 4 km s^{-1}. A spectrum obtained 111,000 km on the sunward side of the coma of C/1996 B2 (Hyakutake) was just outside the optically thick coma. The profile and a Monte Carlo model analysis shows the signatures of the various components: 18 km s^{-1} from H_2O dissociation, 8 km s^{-1} from OH, and the low-velocity line center from thermalized H atoms as shown in Fig. 2. A radiative transfer calculation of all the HST data by *Richter et al.* (2000) showed the detailed effects of multiple scattering of the illuminating solar Lyman-α photons and the progressive saturation of the line center at decreasing distances toward the nucleus of the comet.

4.3. O(^{1}D) λ6300 and Other Forbidden Emissions

Three forbidden O transitions exist in the optical region of the spectrum: the red doublet at 6300.304 and 6363.776 Å (^{1}D–^{3}P) and the green line at 5577.339 Å (^{1}S–^{1}D). These transitions are the result of "prompt" emission, i.e., the atoms are produced directly in the excited ^{1}S or ^{1}D states by photodissociation of the parent molecule. The lifetime of the ^{1}D state is about 130 s, while the ^{1}S state lifetime is less than 1 s. Thus, the three transitions discussed here are excellent tracers of the distributions of their parents because they cannot travel far without decaying. Oxygen atoms that are excited to the ^{1}S state decay to the ground ^{3}P state via the ^{1}D state 95% of the time, while 5% decay directly to the ground state emitting lines at 2977 Å and 2958 Å. Thus, if the green line is present in a cometary spectrum, the red doublet must also be present, although the red doublet can be formed without the green line.

The forbidden O lines can be formed via photoprocesses involving H_2O, CO, or CO_2 as parents. More complex O-bearing species such as HCOOH or H_2CO are unlikely to be the parent because they cannot decay fast enough to produce the observed O(^{1}D) distribution (*Festou and Feldman,* 1981). It is believed that H_2O is the dominant, if not the sole, O(^{1}D) and O(^{1}S) parent out to distances of 10^5 km from the nucleus, beyond which OH becomes the dominant parent. The determination of the parent abundance requires observations of the intensities of the three lines, coupled with accurate understanding of the dissociation rates and branching ratios.

Measuring the intensities of the three lines accurately requires high spectral resolution to resolve the cometary O lines from telluric O lines and other cometary emissions. The resolution needed to resolve the cometary and telluric O lines is dependent on the Doppler shift of the comet with respect to the Earth. For the red doublet, the O(^{1}D) line is situated near cometary NH_2 emissions, but the strong NH_2 lines are generally easy to resolve from the O line when the spectral resolution is sufficient to resolve the cometary and telluric O emissions. The region of the green line is much more difficult. Again, the cometary and telluric lines are Doppler shifted apart. However, the region of the green line is in the middle of the C_2 (1,2) P-branch. Only four observations of the 5577 Å O(^{1}S) line in cometary spectra have been reported: Observations of Comets C/1983 H1 (IRAS-Araki-Alcock) (*Cochran,* 1984) and C/1996 B2 (Hyakutake) (*Morrison et al.,* 1997) relied on high spatial resolution in addition to high spectral resolution; observation of Comet 1P/Halley (*Smith and Schempp,* 1989) relied on extremely high spectral resolution plus modeling; and *Cochran and Cochran* (2001) reported an unequivocal detection of the O(^{1}S) line in spectra of C/1994 S4 (LINEAR) in a comet that was severely depleted in C_2, making the contamination issue go away.

Cochran and Cochran computed the intensity ratio of the red doublet lines and found it to be 3.03 ± 0.14, in excellent agreement with the ratio predicted by the Einstein A-values of *Storey and Zeippen* (2000). Accurate measurement of the ratio of the green line intensity to the sum of the intensities of the red doublet lines can then be used to discriminate between parent species. The values that have been reported [0.22–0.34 for IRAS-Araki-Alcock (*Cochran,* 1984), 0.12–0.15 for Hyakutake (*Morrison et al., 1997*), 0.05–0.1 for Halley (*Smith and Schempp*, 1989), and 0.06 ± 0.01 for LINEAR (*Cochran and Cochran,* 2001)] all point

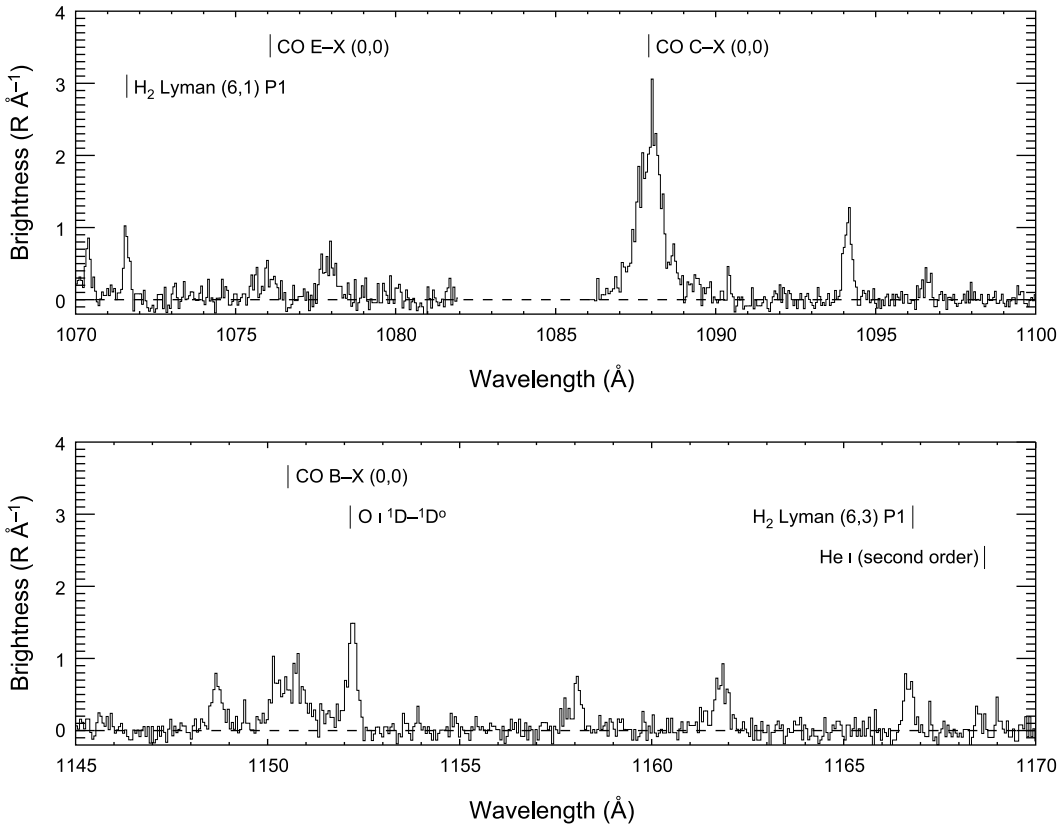

Fig. 3. FUSE spectrum of Comet C/2001 A2 (LINEAR) obtained beginning 2001 July 12.58 UT (from *Feldman et al.,* 2002). Two of the fluorescently excited H_2 lines are identified as well as the CO bands and atomic emissions that lie in this spectral region. A number of detected features remain unidentified.

to H_2O as the dominant parent in the production of the forbidden O lines. However, Cochran and Cochran argue, on the basis of line widths, that H_2O cannot be the sole parent of the O(^{1}D).

With the assumption that most of the O(^{1}D) is produced from the dissociation of H_2O, then the line at 6300 Å can be used to measure the H_2O production rate. This line is more accessible to most detectors than the OH bands of the UV, making its observation an important tool for measuring the H_2O production. Enthusiasm for using measurements of the 6300 Å line must be tempered by an understanding of the limitations. First, there is the issue of the blending of the line with both the telluric O line and with NH_2. In particular, the telluric line is quite variable, so modeling its removal when it is blended with the cometary feature is not easy. High spectral resolution observations of O(^{1}D) has been used on a number of comets (*Magee-Sauer et al.,* 1988; *Combi and McCrosky,* 1991). A far larger set of observations have been obtained at moderate resolution and the O(^{1}D) intensity has been calculated by modeling the contribution of the telluric O(^{1}D) and the cometary NH_2 (*Spinrad,* 1982; *Fink and Hicks,* 1996). *Arpigny et al.* (1987) investigated the effects of spectral resolution on the difficulty of deblending the O(^{1}D) and NH_2 lines and concluded that low spectral resolution can lead to an underestimate of the O(^{1}D) intensity and production rate by about a factor of 2.

Another limitation of using O(^{1}D) as a measure of the H_2O production is that the branching ratios of the reactions that dissociate H_2O are not well determined. *Budzien et al.* (1994) summarized the uncertainties in our knowledge of these branching ratios. Since OH is produced approximately 90% of the time, with O produced approximately 10% of the time, errors in the branching ratio induce a larger uncertainty in our calculation of H_2O production rates from O(^{1}D) than from OH. In addition, while all the OH is a daughter of H_2O, some of the O(^{1}D) is a daughter of the dissociation of H_2O, while some is a product of the subsequent dissociation of OH.

4.4. Molecular Hydrogen

Feldman et al. (2002) recently reported the FUSE observation of three P1 lines of the H_2 Lyman series that are excited by the accidental coincidence of the solar Lyman-β line with the P1 line of the $B^1\Sigma_u^+$–$X^1\Sigma_g^+$ (6,0) band in the spectrum of Comet C/2001 A2 (LINEAR), shown in Fig. 3. Similar fluorescence has also been seen in the spectra of Jupiter and Mars. Although the strongest of the fluorescent

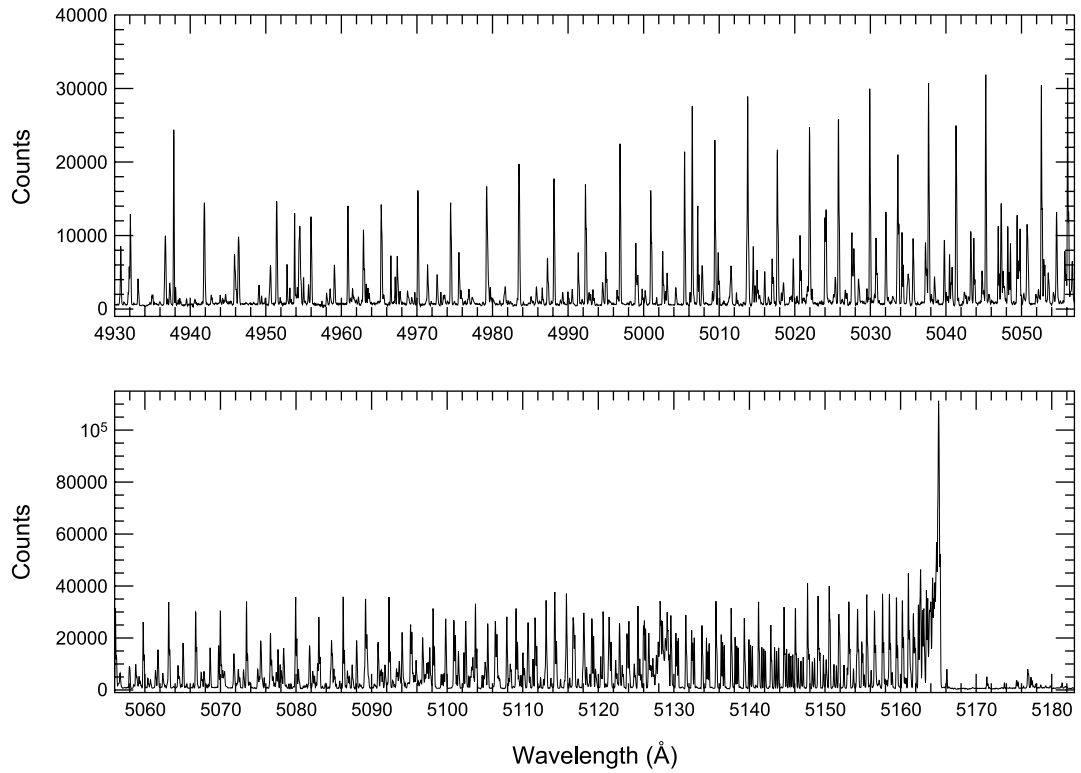

Fig. 4. Spectrum of Comet 122P/deVico showing two-thirds of the C_2 $\Delta v = 0$ band observed at a resolving power $\lambda/\Delta\lambda = 60{,}000$ with the McDonald Observatory 2.7-m 2D-coudé spectrograph. The two panels have different ordinate scalings to better show the details of the spectra. The bluest lines shown at 4932.059 and 4932.139 Å are C_2 (0,0) $R_1(73)$, $R_2(72)$, and $R_3(71)$. Most of the lines shown in the spectrum are attributable to C_2. However, there are some NH_2 and unidentified lines mixed throughout this spectrum.

lines appear near 1600 Å, longer-wavelength spectra of comets from IUE, HST, and sounding rockets have not had sufficient spectral resolution to unambiguously identify H_2 in cometary spectra. The determination of the H_2 column density in the field of view depends strongly on the shape of the solar Lyman-β line, the rotational temperature and outflow velocity of the H_2, and the heliocentric velocity of the comet. Feldman et al. demonstrated that the derived column abundance of H_2 is consistent with H_2O dissociation models but cannot exclude that some of it is produced directly from the nucleus (*Bar-Nun and Prialnik,* 1988) or by solar wind sputtering of dirty ice grains (*Pirronello et al.,* 1983).

5. CARBON-, NITROGEN-, AND SULFUR-CONTAINING RADICALS

5.1. C_2

There are two principal band systems of C_2 that are observed in the optical spectra of comets. These are the Swan, or $d^3\Pi_g$–$a^3\Pi_u$, system, and the Phillips, or $A^1\Pi_u$–$X^1\Sigma_g^+$, system. The Swan system was the first molecule identified in a cometary spectrum and is dominant in the green, orange, and red region of the spectrum; the Phillips bands are important in the near-IR and IR. In addition, the C_2 $D^1\Sigma_u^+$–$X^1\Sigma_g^+$, or Mulliken, system has been detected in the UV, despite the fact that the Mulliken $\Delta v = 0$ band's g-factor is about 40 times smaller than that of the Swan $\Delta v = -1$ band sequence [see Fig. 2 of *A'Hearn* (1982)].

In comparison to CN and other cometary molecules, much higher C_2 vibration-rotation levels are excited (see Fig. 4). Indeed, vibration-rotation levels as high as J = 109 have been detected (*Cochran and Cochran,* 2002). This high-J distribution occurs because C_2 is a homonuclear molecule with no permanent dipole moment so that vibrational and rotational electric dipole transitions within an electronic state are forbidden. Thus, the rotational excitation temperature of the C_2 coma would be approximately the color temperature of the Sun (T = 5800 K) in the absence of any mechanism for cooling the rotational temperature. This mechanism does exist, however, in the form of interactions with other electronic states.

The rotational excitation temperature (T_{rot}) of the coma can be measured by observing the Swan bands at high spectral resolution. Such observations have generally yielded $T_{rot} \sim 3000$ K. *Lambert et al.* (1990) observed Comet Halley and found that the C_2 gas could not be described by a single rotational temperature. They found that the lower rotational levels (J < 15) could be fit with $T_{rot} \sim 600$ K, while higher levels required $T_{rot} \sim 3200$ K. Indeed, when the contribution of the hotter population is accounted for, the low-J levels

yield T_{rot} = 190 K. *Krishna Swamy* (1997) has shown that these results can be understood in detail by the inclusion of many more transitions in models of the photolysis of C_2.

C_2 emissions can be detected at large distances from the nucleus, implying a large scale length for its production. However, it has long been noted that the distribution in the inner few thousand kilometers of the coma is essentially constant. This flat distribution is inconsistent with a simple parent/daughter production for C_2. *Jackson* (1976) was the first to suggest that C_2H_2 was the grandparent of C_2, with an intermediate decay of the C_2H_2 to C_2H + H. Using long-slit CCD observations of Comet Halley, *O'Dell et al.* (1988) also concluded that C_2 must be the product of the decay of two precursors. Using a multigeneration Haser model, they found that the data can be fit with parameters between R_1 = 12,000 km, $R_1/R_2 = 3$, and $R_2/R_3 = 0.8$; to R_1 = 17,000 km, $R_1/R_2 = 1.5$, and $R_2/R_3 = 0.12$, where R_1, R_2, and R_3 are the grandparent, parent, and daughter destruction scale lengths, respectively.

Combi and Fink (1997) further investigated a solution for the flat inner profile of the C_2 gas. They also used a three-generation dissociation model, but theirs differed from that of *O'Dell et al.* (1988) by the inclusion of ejection velocities resulting from the excess energy of the photodissociations. They found that, as long as the ejection velocities are greater than 0.5 km s^{-1}, the excess energy imparted during the various dissociations will cause a filling in of the "hole" in the profile, resulting in a profile that is no longer flat in the inner coma. They argued that typical heavy molecules produce ejection velocities in excess of 1 km s^{-1}, so a three-generation photodissociation is unlikely the parent process for the production of C_2. Instead, they suggest that a CHON grain halo with a size of 10^4 km is responsible for the production of X–C_2 (X is some unknown species), which in turn is photodissociated on a scale of several times 10^4 km to produce the C_2. This process can proceed with little or no excess energy.

New laboratory data and *ab initio* calculations (*Sorkhabi et al.,* 1997) would seem to allow for the original thesis of *Jackson* (1976), that the grandparent of C_2 is C_2H_2, while the direct parent is C_2H. *Sorkhabi et al.* (1997) obtained laser-induced fluorescence spectra of C_2 ($X^1\Sigma_g^+$) radicals produced during 1930 Å laser photolysis of C_2H_2. They used these observations along with calculations to match the spectrum of the C_2 Mulliken system in HST observations of Comet C/1996 B2 (Hyakutake).

5.2. CN

There are two CN electronic band systems that can be observed in the optical in cometary spectra. These are the "violet" system ($B^2\Sigma^+$–$X^2\Sigma^+$) and the "red" system ($A^2\Pi$–$X^2\Sigma^+$). The violet system is one of the most prominent features in cometary spectra and is seen in most comets with heliocentric distances less than 3 AU. It has been detected in Comets 1P/Halley and C/1995 O1 (Hale-Bopp) at distances greater than 4 AU and in the Centaur (2060) Chiron at 11.26 AU (*Bus et al.,* 1991). Despite its spectral prominence, its parent must have less than 1% of the abundance of H_2O.

Because the violet system is a Σ–Σ transition, only P- and R-branches are permitted and J < 20 is generally observed. This, coupled with the density of absorption features in the solar spectrum at the wavelength of the Δv = 0 bands at 3883 Å, makes it necessary to account for the Swings effect when converting observed band flux to column density. Results of calculations of the change in the g-factor with changing heliocentric radial velocity have been given by *Tatum and Gillespie* (1977), *Tatum* (1984), and others. The solar spectrum shows strong CN Σ–Σ absorption so that the g-factor reaches a minimum at zero heliocentric radial velocity (at perihelion). While the cometary CN violet band does not disappear entirely at perihelion, it becomes quite weak. The red system is generally much more spread over wavelength and does not appear as such an obvious band.

High spectral resolution allows the isotopic features of CN to be clearly resolved from the weak, high-order non-isotopic features. Thus, studies of CN with high spectral resolution have been used to derive $^{13}C/^{12}C$ values that are essentially the solar value for several comets (*Kleine et al.,* 1994, 1995; *Lambert and Danks,* 1983; *Lambert et al.,* 1990). High spectral resolution, coupled with high signal/noise, have allowed *Arpigny et al.* (2003) to determine ^{15}N ^{14}N in a number of comets. They found a value that is a factor of 2 higher than the value from the Earth's atmosphere.

Although the identification of the violet system as CN has been known since the earliest days of comet spectroscopy, the identification of the parent is still in doubt. The Haser (or radial) scale length of the CN parent is on the order of 2×10^4 km at 1 AU. A potential parent, HCN, is observed in the millimeter portion of the spectrum, but it is still uncertain whether HCN is a minor parent or a dominant parent of CN. *Bockelée-Morvan and Crovisier* (1985) argued that the CN distribution is inconsistent with HCN as a dominant parent unless the coma expansion velocity was much lower than generally assumed. In contrast, direct comparison of the distribution of HCN and CN using more recent millimeter observations have shown that there is sufficient HCN to be a dominant parent of CN (*Ziurys et al.,* 1999) and that the HCN and CN are distributed similarly within the coma (*Woodney et al.,* 2002).

Festou et al. (1998) asserted that HCN contributes at the percent level to the production of CN. They found that a best case for a parent for CN has a lifetime of 3.5×10^4 s at 1 AU with a velocity of 1–2 km s^{-1}. They concluded that this is consistent with C_2N_2 as the dominant parent. *Bonev and Komitov* (2000) fit the CN scale lengths and concluded that C_2N_2 is the sole parent for CN.

5.3. C_3

The first detection of the emission band that we now know to be C_3 was in 1881. However, the tentative identification of the band as C_3 was not made until 1951 (*Douglas,* 1951). C_3 is a relatively unstable molecule, making its study difficult. Until its identification, the band was known sim-

ply as the "4050-Å Group." The main part of the band lies between 3900 and 4140 Å with a maximum at 4050 Å and an additional peak, not well defined, at 4300 Å. However, careful examination of cometary spectra shows lines attributable to this band from ~3350 to 4700 Å.

C_3 is a linear, symmetric molecule containing equal-mass nuclei. The band has been identified as an $\tilde{A}^1\Pi_u$–$\tilde{X}^1\Sigma_g^+$ electronic transition. R-branch bandheads at 4072 and 4260 Å can be assigned to the (1,0,0)–(1,0,0) and (0,0,0)–(1,0,0) bands respectively. The density of the lines results in a pseudo-continuum from C_3. For all Σ states of the molecule, every second line is missing. In other states, one member of the e/f-parity doublet of each rotational level is missing, although all rotational levels are represented (*Tokaryk and Chomiak,* 1997). The complexity of the spectrum and the difficulty of exciting C_3 in the laboratory have resulted in many missing identifications of lines. In addition, the density of lines has made it impossible to resolve all the individual lines. Recently, observations of cometary C_3 were used to derive a new dipole moment derivative (dμ/dr) of approximately 2.5 Debye $Å^{-1}$ for this band system (*Rousselot et al.,* 2001).

The parent of C_3 is unknown. Chemically plausible parents, such as C_3H_4 and C_3H_8, are not detected in cometary spectra. Either of these would produce C_3 in a multigenerational process and many of the photolysis rates for such reactions are very uncertain. Observations of the distribution of C_3 gas in the comae of comets suggests that the parent must have a short scale length, on the order of 3×10^3 km (*Randall et al.,* 1992). It is unlikely that the long-chain C molecules seen in the interstellar medium are parents for C_3 since these long-chain C molecules are believed to have alternating single and triple bonds that would more likely break to produce C_2 than C_3. The photodestruction of C_3 results in the production of a C_2 molecule and a C atom.

5.4. CH

The CH (0,0) $A^2\Delta$–$X^2\Pi$ band has its peak at 4314 Å and appears in cometary spectra as a weak band. Two factors contribute to this weak feature of interest: (1) The oscillator strength is small, $\sim 5 \times 10^{-3}$; and (2) the lifetime against photodissociation at 1 AU is between 35 and 315 s (*Singh and Dalgarno,* 1987). The former implies that even a very weak feature is the result of a significant column density. The latter means that wherever the CH is detected in the coma, the parent must be close by. Thus, CH can be used as a tracer of the parent distribution.

The probable parent of CH is CH_4. Methane will first decay into CH_2 (CH_3 is highly unstable) and then into CH. The detection of CH in the optical is far simpler than the detection of CH_4 in the IR so there is a significantly larger database of CH detections than CH_4 detections.

The (0,0) $B^2\Sigma^-$–$X^2\Pi$ band has also been detected at high spectral resolution at 3886 Å. This band cannot be resolved from CN at lower resolution. It is necessary to be aware of this band, however, when computing models of $^{12}CN/^{13}CN$, since some of the CH lines are coincident with the weaker CN lines.

5.5. NH and NH_2

The (0,0) $A^3\Pi_i$–$X^3\Sigma^-$ band of NH occurs between 3345 and 3375 Å. It was first detected in the spectrum of Comet Cunningham (*Swings et al.,* 1941) and is generally the only NH band seen. This band shows an R- and P-branch but the Q-branch is absent or weak. *Kim et al.* (1989) showed that the spectrum can be explained completely on the basis of pure resonance fluorescence without any collisions.

Emission lines of NH_2 have been detected throughout a region from ~3980 Å to well past 1 μm (*Cochran and Cochran,* 2002). These lines belong to the $\tilde{A}^2A_1$–$\tilde{X}^2B_1$ electronic transition, along with transitions between the high vibronic levels and the ground state of the $\tilde{X}^2B_1$ electronic band [e.g., $(0,13,0)\tilde{X}^2B_1$–$(0,0,0)\tilde{X}^2B_1$]. NH_2 is an asymmetric top molecule, with a linear upper level and a lower level bent at an angle of 103°, making its spectrum quite complex and irregular.

It is widely believed that NH_3 is the parent for NH_2, which decays, in turn, into NH. However, until recently, NH_3 had not been detected in cometary spectra. *Palmer et al.* (1996) first detected NH_3 in the radio spectrum of C/1996 B2 (Hyakutake) and it has now also been detected in the radio spectrum of C/1995 O1 (Hale-Bopp) (*Bird et al.,* 1997) and the IR spectrum of 153P/Ikeya-Zhang (*Magee-Sauer et al.,* 2002). Other potential parents include N_2H_4 and CH_3NH_2.

Prior to the detection of NH_3, the chemical reaction pathway was argued on the basis of the observed scale lengths of the various species. However, there has been much disagreement on the values relevant to each species. Typically, the g-factors for NH_2 of *Tegler and Wyckoff* (1989) are used. *Arpigny* (1994) pointed out that this g-factor calculation is off by a factor of 2 because the structure of the NH_2 bands means that a single band when the linear band notation is used (typical in past cometary work) only samples either odd or even K_a lower levels. *Cochran and Cochran* (2002) advocated converting to using the bent band notation adopted by the physicists. Under that notation, the linearly denoted (0,8,0) Π band is a part of the bent notation (0,3,0) band and the (0,8,0) Φ band is part of the (0,2,0) band. The bent notation bands contain both odd and even K_a lower levels. It is generally believed that the parent of NH_2 has a relatively short scale length, on the order of $\sim 4 \times 10^3$ km (*Krasnopolsky and Tkachuk,* 1991; *Fink et al.,* 1991). The destruction scale length is a few times 10^4 km.

Kawakita et al. (2001b) have derived new g-factors for five of the bands (in the linear notation) and find values smaller than those of *Tegler and Wyckoff* (1989) by factors of 2.7 to 6.4. Korsun and Jockers (2002) have applied these g-factors to NH_2 filter images and shown that the derived NH_2 production rate is consistent with NH_3 as the parent.

Kim et al. (1989) have calculated NH fluorescence efficiencies incorporating the Swings effect. Part of the prob-

lem with defining scale lengths for NH is a paucity of data coupled with the difficulty of determining the atmospheric extinction at the wavelength of NH. Parent scale lengths range from 1–5 × 10^4 km. *Schleicher and Millis* (1989) argue reasonably convincingly for the longer of these values. Most datasets are not very sensitive to the destruction scale length used, but it is generally agreed to be about 2 × 10^5 km. *Feldman et al.* (1993) used spectrophotometric spatial profiles of OH and NH emission derived from observations of Comet 1P/Halley made by the Soviet-era ASTRON satellite to derive the relative NH_3 abundance with a nearly model-independent analysis.

All the observations suggest that about 95% of the photodissociations of NH_3 produce NH_2 and that very little of the NH comes directly from NH_3. Using the various parameters found in the literature, there is general agreement that the abundance of NH_3 in the nucleus is about 0.5% that of H_2O for all comets, if NH_3 is the sole parent of NH_2 and NH.

Recently, *Kawakita et al.* (2001a) have utilized high-resolution NH_2 spectra of Comet C/1999 S4 (LINEAR) to model the ortho-to-para ratio and to derive a spin temperature for NH_3. They found a temperature of 28 ± 2 K, assuming that the NH_2 arises from pure fluorescence excitation of NH_3.

5.6. CS

Ultraviolet emission from carbon monosulfide (CS) and atomic sulfur was first reported in rocket spectra of Comet West (C/1976 V1) by *Smith et al.* (1980). The (0,0) band of the $A^1\Pi$–$X^1\Sigma^+$ system of CS at 2576 Å is the strongest of four bands of this system lying between 2500 and 2700 Å and has been detected in nearly all IUE and HST comet spectra. More recently, CS has also been detected in the radio (*Biver et al.,* 1999). *Jackson et al.* (1982) analyzed both high- and low-dispersion IUE spectra of Comet Bradfield (C/1979 Y1), concluding that the likely parent was CS_2 with an extremely short photodissociation lifetime of ~100 s at 1 AU. They also found that the band shape was indicative of a 70-K rotational temperature, that the production rate of the parent was about 0.1% that of water near 1 AU, and that this ratio decreased with increasing heliocentric distance. This latter behavior has been seen in all the comets observed by IUE over a significant range of r and also in the radio observations of Comet Hale-Bopp (C/1995 O1) (*Biver et al.,* 1999). *Jackson et al.* (1982) suggested that CS_2 could also account for all the observed S I emission at 1814 Å, although it was later shown that H_2S was a more important source of S than CS_2 (*Meier and A'Hearn,* 1997). Sulfur-bearing species are discussed in section 4.5 of *Bockelée-Morvan et al*. (2004). *Jackson et al.* (1982), in discussing the photodissociation of CS_2, noted that laboratory measurements using a source at 1930 Å produced an abundant amount of S(^{1}D) atoms in addition to ground state ^{3}P atoms. Sulfur in the ^{1}D state was detected by its transition at 1667 Å in GHRS spectra of Comet Hyakutake (C/1996 B2) (*A'Hearn et al.,* 1999).

Further IUE observations and laboratory data led *Jackson et al.* (1986) to revise the CS_2 lifetime at 1 AU to ~500 s, and this seemed to be consistent with the limited spatial information available from low-dispersion IUE spectra. However, high-dispersion spectra of 1P/Halley showed the band shape to be quite different from previously observed comets, with the R-branch blueward of the band head much enhanced over the redward P,Q branches, in contradiction with solar fluorescence models. Attempts to model this band with two components along the spectrograph line of sight, the first in statistical equilibrium near the nucleus, and the second in fluorescence equilibrium for distances greater than ~1000 km from the nucleus, have been only partially successful in reproducing the observations (*Prisant and Jackson,* 1987; *Krishna Swamy and Tarafdar,* 1993).

In the HST era, spectra of the CS (0,0) band at resolution comparable to that of the IUE high-dispersion mode ($\Delta\lambda$ = 0.8 Å) have not been obtained, precluding a resolution of this problem. In one area, though, spatial imaging with STIS has led to a more reliable estimate of the CS parent lifetime of ~1000 s (*Feldman et al.,* 1999).

Another potential source of CS in the coma is OCS, detected in the radio in recent comets in comparable abundance to CS_2 (see *Bockelée-Morvan et al.,* 2004). However, the primary dissociation path of OCS is to CO and S (*Huebner et al.,* 1992) so that the contribution to the CS abundance is minor. Other S-bearing parent molecules identified in the radio are H_2S and SO_2, the former being the principal S species in the cometary ice (see *Bockelée-Morvan et al.,* 2004). *Kim and A'Hearn* (1991, 1992) have given spectroscopic limits on the dissociation products SH and SO, although the latter has been detected in the radio in Comet Hale-Bopp (*Bockelée-Morvan et al.,* 2000). Finally, we note that *Irvine et al.* (2000) have reported the detection of NS in Comet Hale-Bopp, although its origin remains unknown.

6. ATOMIC BUDGET OF THE COMA

With the exception of CO and CO_2, solar photodissociation rates are significantly higher than the rates for photo- or solar wind ionization of the principal molecular constituents of the coma (*Huebner et al.,* 1992). Thus, the end products of the molecular species will be predominantly the constituent atoms, H, O, C, N, and S, and their corresponding ions. The neutral atomic species all have their principal resonance transitions in the vacuum UV in a wavelength range amenable to spectroscopic observations by IUE and HST (see Table 2). H I Lyman-α observations, both spectroscopic and imaging, are discussed in section 4.2 above and in *Combi et al.* (2004). Because of the large scale lengths against ionization for these species, the atomic coma can extend to millions of kilometers from the nucleus and images in Lyman-α show the atomic hydrogen corona to be the largest object in the solar system, often attaining a size of ~0.1–0.2 AU.

The resonance transitions of atomic carbon and oxygen were first detected in rocket observations of Comet Kohou-

TABLE 2. Principal resonance transitions of cometary atoms and ions.

Species	Transition	Wavelength (Å)
H I	$^2P^o$–^2S	1216
O I	$^3S^o$–^3P	1302–06
C I	$^3D^o$–^3P	1561
	$^3P^o$–^3P	1657
N I	^4P–$^4S^o$	1134
	^4P–$^4S^o$	1200
S I	^3P–$^3S^o$	1807–26
O II	^4P–$^4S^o$	834
C II	^2S–$^2P^o$	1037
	^2D–$^2P^o$	1335
N II	$^3D^o$–^3P	1085
S II	^4P–$^4S^o$	1250–59

tek (C/1973 E1) (*Feldman et al.,* 1974; *Opal et al.,* 1974), the latter also providing objective grating images of the C and O comae. Because of the large heliocentric velocity at the time of the observation, the O I λ1302 multiplet was Doppler shifted away from the solar O I line and the excitation was attributed to "Bowen fluorescence" of solar Lyman-β (*Feldman et al.,* 1974). Similarly, C I λ1657 and the CO Fourth Positive bands were shown to be subject to a large "Swings effect" (Feldman et al., 1976). From similar observations made of Comet West (C/1975 V1), *Feldman and Brune* (1976) showed that the C could be accounted for as the dissociation product of the CO simultaneously measured. Comet West had an unusually high CO abundance and so it was a surprise when Comet Bradfield (C/1979 Y1), observed by IUE, showed a large C emission despite a much smaller relative CO production rate (*A'Hearn and Feldman,* 1980). IUE used a much smaller aperture than had the earlier rocket spectrometers, and *Festou* (1984) considered whether the additional C could be indicative of the presence of many other C-bearing species near the nucleus, many of which were subsequently discovered in later comets. Festou also postulated that the atomic inventory, independent of the details of the molecular parentage and assuming that all the photons could be collected from the extended coma, would be a strong indicator of cometary diversity.

In addition to the resonance multiplet of O I, the intercombination doublet at 1356 Å has been observed in a few coma spectra (*Woods et al.,* 1987; *McPhate et al.,* 1999). Because the g-factor for this transition is so small, the excitation source has been attributed to photoelectrons, analogous to the excitation in planetary atmospheres (*Cravens and Green,* 1978). Electron impact excitation may also contribute to the observed CO Cameron band emission (*Weaver et al.,* 1994).

Atomic sulfur was first identified in the spectrum of Comet West by *Smith et al.* (1980), who also obtained an objective image of the S I λ1813 multiplet. This emission has been detected in nearly every comet observed since then by IUE or HST, and most of the observations show the 1807 Å component, the transition connecting to the lowest ground-state level, to be saturated. *Azoulay and Festou* (1986) first treated opacity effects in order to properly extract S production rates and concluded that CS_2 was insufficient to account for the amount of S observed and that OCS was likely the primary parent. *Meier and A'Hearn* (1997), analyzing a much larger database of S observations, came to a similar conclusion but identified the primary parent as H_2S, which had recently been detected in radio observations.

Two other S multiplets are occasionally detected in comets that are observed at small heliocentric velocity (<10 km s^{-1}), at 1429 and 1479 Å. These transitions are also optically thick near the nucleus. A particularly nice example of these emissions is seen in the long-slit spectrum of Comet Hale-Bopp obtained from the rocket experiment of *McPhate et al.* (1999) (Fig. 5). This spectrum also shows how the relative intensities of the three components of the S I λ1813

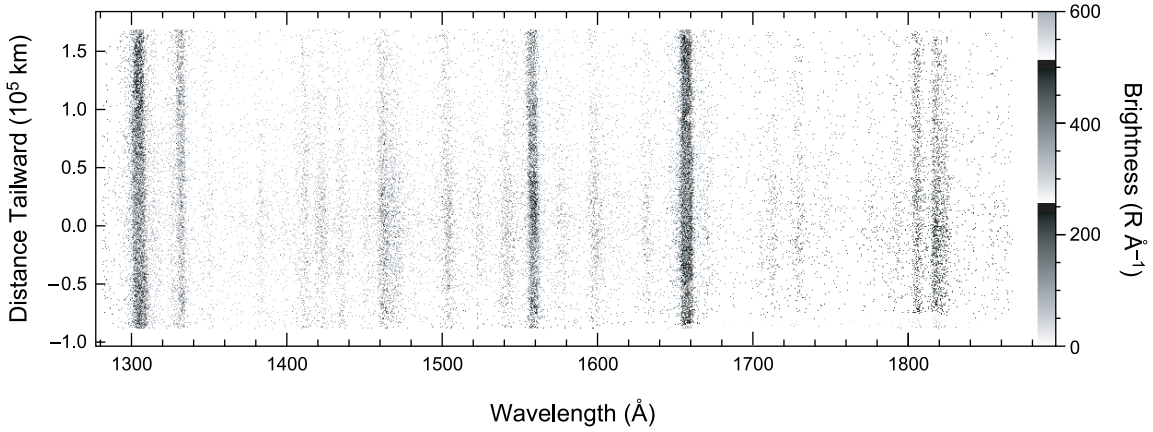

Fig. 5. Long-slit spectral image of Comet Hale-Bopp acquired on 1997 April 6.16 UT. The long axis of the slit was oriented along the Sun-comet line and the slit was offset 20" from the nucleus. The Sun is down in this image. Each pixel is 0.6 Å × 0."8 and subtends 800 km at the comet. The emission features are identified in Fig. 6. From *McPhate et al.* (1999).

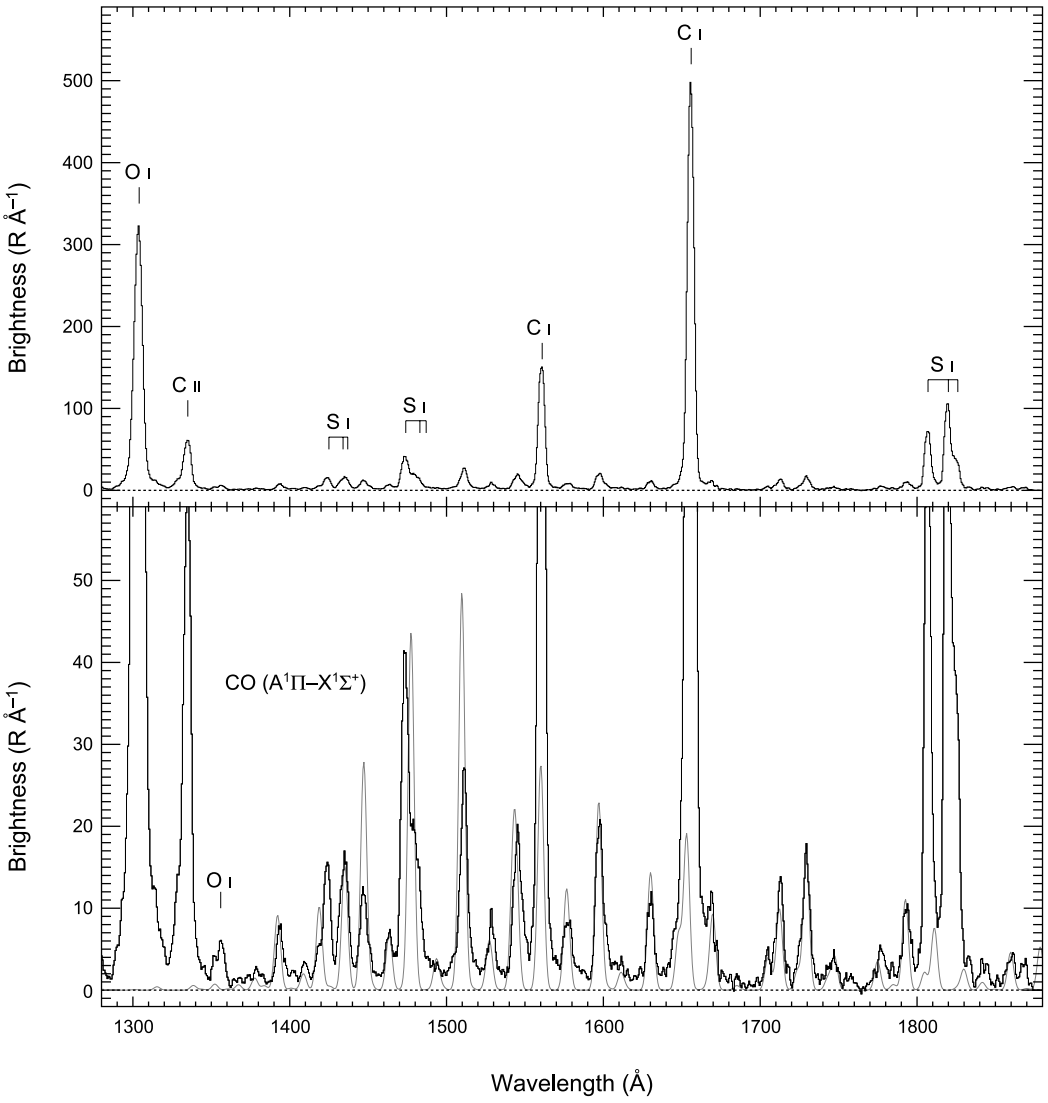

Fig. 6. Full-slit average spectrum derived from the data of Fig. 5. The top frame identifies the stronger atomic emissions while the bottom frame, expanded in scale, shows the rich molecular spectrum of CO. The gray line is a modeled optically thin CO Fourth Positive band spectrum. From *McPhate et al.* (1999).

multiplet vary with distance from the nucleus, the line ratios approaching optically thin values at 150,000 km (Fig. 6).

In contrast to the other atomic species, little is known about atomic nitrogen in the coma. Its principal resonance transition at 1200 Å has never been detected, presumably due to the weakness and narrowness of the solar exciting lines and its close proximity to the very strong H I Lyman-α line. *Weaver et al.* (2002) report the detection of the strongest member of the N I λ1134 multiplet in the FUSE spectrum of Comet C/2001 A2 (LINEAR), but this identification needs to be confirmed.

7. SODIUM IN COMETS NEAR 1 AU

Recognition of cometary Na D-line emissions at 5890/5896 Å dates back to visual observations of Comets C/1882 F1 and C/1882 R1 (*Levin,* 1964) and Comet C/1910 A1 (*Newall,* 1910). For the latter comet, handheld prism observations indicated that the tailward extent of the Na emission exceeded that of the C_2 Swan band for this comet. Although Na is a minor species in all atmospheres where it has been detected [Io (*Brown and Chaffee,* 1974), Mercury (*Potter and Morgan,* 1985), Moon (*Potter and Morgan,* 1988)], it has nonetheless been useful because trace amounts of Na are easily observed because of the large ocillator strength in the D-lines and their placement at the peak wavelength of solar radiation.

The curious behavior of Na and its emission results from the strong interaction with solar radiation. The solar spectrum contains two strong Na absorption lines that modulate the fluorescence of Na atoms in the solar system depending upon their heliocentric velocity. At 1 AU from the Sun, strong fluorescence in the D-lines produces a large radiation pressure acceleration, which varies from about

3 cm s^{-2} for Na atoms at rest with respect to the Sun (and seeing the bottom of the solar lines) to more than 50 cm s^{-2} for Na atoms Doppler shifted to the nearby continuum.

The first Na studies were largely confined to Sun-grazing comets, perhaps most notable of which was Comet Ikeya-Seki (C/1965 S1), with perihelion q = 0.04 AU, and for which Na emission was not seen for heliocentric distances r > 0.6 AU (*Bappu and Sivaraman,* 1969). Based on observations of this comet by *Preston* (1967) and *Spinrad and Miner* (1968), *Huebner* (1970) argued that under these harsh conditions the intensity of Na D emission could be accounted for by Na atoms embedded within micrometer-sized refractory silicate material having a high latent heat of vaporization. *Preston* (1967), in particular, noted that a whole set of metallic species in addition to Na were detected spectroscopically. These emission lines were tabulated by *Slaughter* (1969). Because of the short photoionization lifetime of Na atoms close to the Sun and the substantial tailward extent of the Na emission (~10^3 km), the early studies of the Sun-grazing comets (*Spinrad and Miner,* 1968; *Huebner,* 1970) equated the tailward extent as being indicative of the lifetimes of parent refractory grains. These studies, however, neglected the very large radiation pressure acceleration on Na atoms. In addition, it has since been found that the photoionization lifetime (*Huebner et al.,* 1992; *Combi et al.,* 1997) may be up to three times longer than believed at the time.

Observations of Na emission near and beyond 1 AU have been limited to a few bright, active comets. The Na in Comet Kohoutek C/1973 E1 (q = 0.18 AU) was seen at least out to heliocentric distance of 0.47 AU (*Delsemme and Combi,* 1983). The first interpretation of Na D emission at distances beyond 1 AU was by *Oppenheimer* (1980) in Comet West (C/1975 V1) at 1.4 AU; Oppenheimer concluded that the Na was trapped in molecules within the volatile ice component. He reasoned that only with Sun-grazing comets would the refractory grain component be hot enough to liberate Na, either in elemental or molecular form.

Delsemme and Combi (1983) reported that the Na spatial profile in Comet Kohoutek had its brightest pixel at the same location as the dust continuum, whereas the other gas species (C_2, CN, and NH_2) were all displaced sunward, suggesting some connection of Na with the dust. *Combi et al.* (1997) reported a detailed model analysis of spatial profiles of Na from long-slit spectra in non-Sun-grazing comets [Bennett (C/1969 Y1), Kohoutek (C/1973 E1), and 1P/Halley] and identified two types of spatial signatures. There was a relatively stable point source of Na, produced directly from the nucleus or a short-lived parent, as well as an extended source seen mainly on the tailward side. The latter had a larger production rate and varied by factors of a few compared with the nucleus source on timescales as short as a day. They also noted some spatial similarities in Halley between the extended Na distribution and ion profiles but not with the dust. This combined with the large variability led them to suggest a possible role for some plasma process for the extended source.

Because of its extremely large overall gas production rate, a spectacularly bright and long Na tail was imaged in Comet Hale-Bopp (C/1995 O1) by *Cremonese et al.* (1997) and *Wilson et al.* (1998). Modeling analysis of these images and further spectroscopic observations (*Brown et al.,* 1998; *Rauer et al.,* 1998; *Arpigny et al.,* 1998) showed that the observed distribution of Na in the tail could be explained by a nucleus or near-nucleus source of Na at a production rate that is less than 0.3% of what would be expected based on solar abundances of Na compared with O. This is in fact the same level as the nucleus or near-nucleus source for Na identified by *Combi et al.* (1997) in Comet Halley and seen in Comets Bennett and Kohoutek. Therefore, the gaseous Na seen in non-Sun-grazing comets does not represent the bulk of Na in comets, which is mostly bound to the refractory component and was seen in the dust mass spectra of 1P/Halley (*Jessberger and Kissel,* 1991).

Unlike the extended source of Na in Halley, inner coma measurements of Na in Comet Hale-Bopp showed an extended source component that appeared to be associated with the asymmetric dust distribution (*Brown et al.,* 1998). Brown et al. found that roughly half the Na was produced from the nucleus source and half from an extended source that roughly followed the r^{-2} distribution of the asymmetric dust coma and did not resemble either the spatial or velocity distribution seen in simultaneously observed H_2O^+ ions. Observations of Na in future bright comets are required in order to answer the question of the nature of the extended source.

8. IONS

8.1. Molecular Ions

Photolytic processes and chemical reactions will ionize molecules in the comae of comets and, as a result, various molecular ions have been detected in cometary spectra. In the UV and optical, these include CH^+, CO^+, CO_2^+, H_2O^+, N_2^+, and OH^+. Ions have now been detected in the radio spectrum of Comet C/1995 O1 (Hale-Bopp), including HCO^+ (Wright et al., 1998), H_3O^+, and CO^+ (*Lis et al.,* 1999). The ions show a very different distribution in the coma than do neutrals since the ions are accelerated tailward by the solar wind. Thus, the ionic species are often called "tail" species. However, it should be noted that many are observed relatively close to the nucleus of the comet, a good illustration being obtained from long-slit spectra of CO^+ and CO_2^+ in Comet 1P/Halley given by *Umbach et al.* (1998).

The predominant processes for the production of ions are photodissociation (e.g., $H_2O + h\nu \rightarrow OH^+ + H + e$) and photoionization (e.g., $H_2O + h\nu \rightarrow H_2O^+ + e$) (*Jackson and Donn,* 1968). Within the collisional zone (the inner few thousand kilometers of the coma for moderately bright comets), ions can be produced by charge exchange with solar wind protons, electron impact ionization, charge transfer reactions, and proton transfer reactions.

The transitions of CO^+ that are seen in the blue/UV region of the spectrum arise from the first negative bands

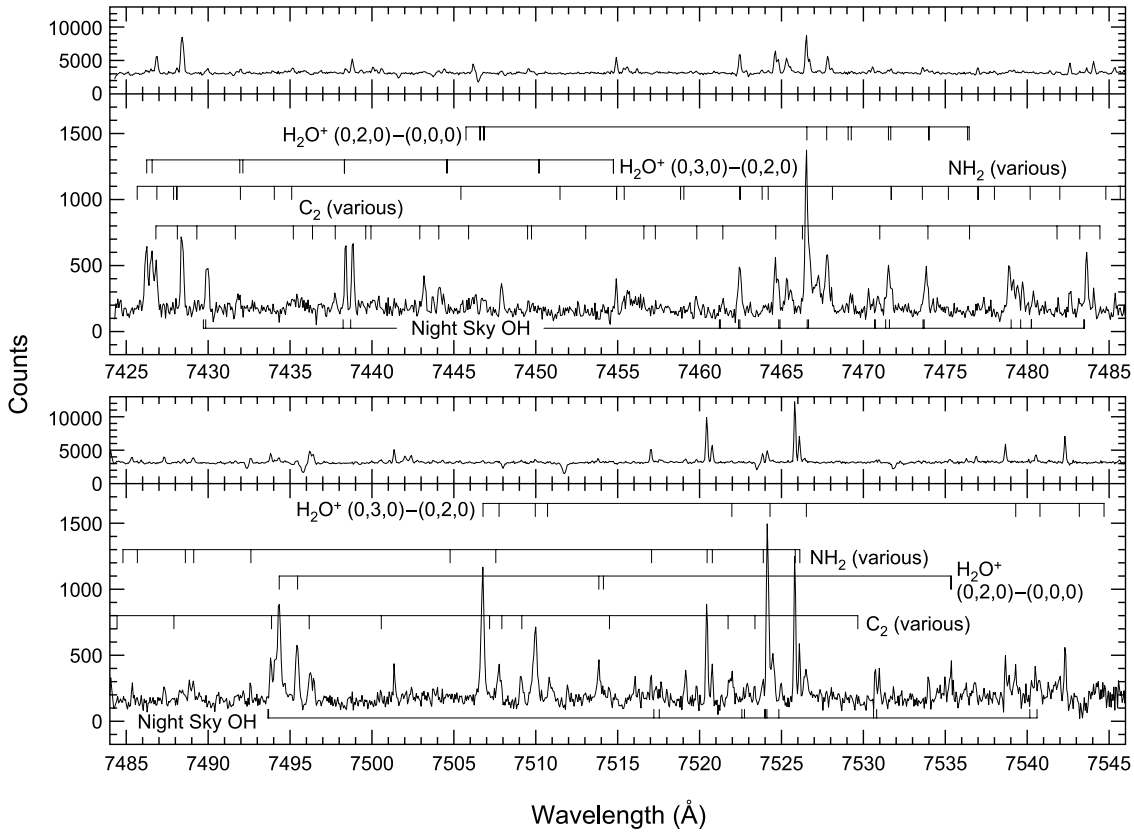

Fig. 7. Spectrum of Comet 153P/Ikeya-Zhang, recorded 15,000 km tailward from the optocenter, illustrating a well-developed ion tail. The narrow panel for each half of the order is the optocenter spectrum while the wide panel is the tail spectrum. All lines from two H_2O^+ bands are marked, along with lines of NH_2 and C_2 (Phillips). Not all the marked ionic lines are present; only the lower J-values appear in the spectrum. Comparison of the tail and the optocenter spectra show the increased strength of the ionic lines relative to the neutrals. The solar continuum has not been removed from either spectrum. This spectrum was obtained with the McDonald Observatory 2D-coudé at R = 60,000.

($B^2\Sigma$–$X^2\Sigma$) and the comet-tail bands ($A^2\Pi$–$X^2\Sigma$). The comet-tail bands show two peaks that are due to the $\Pi_{1/2}$ and $\Pi_{3/2}$ branches. Generally, the (2,0) and (3,0) comet-tail bands are the strongest bands observed. The comet-tail transitions are responsible for the blue appearance of the ion tail in color images of comets.

The presence of the CO^+ bands in cometary spectra has led to the belief that CO is generally present at the few percent level in cometary nuclei. CO^+ emissions are seen in cometary spectra to heliocentric distances greater than 5 AU (*Cochran and Cochran,* 1991). *Magnani and A'Hearn* (1986) have calculated fluorescence efficiencies for most of the comet-tail bands accounting for the Swings effect, which should be a factor since there are relatively few excited levels and the solar spectrum is dense in the blue.

Another ion that appears prominently in the red part of the spectrum is H_2O^+. Although it has been observed in cometary spectra for a long time, it was only identified for the first time in 1974 in spectra of Comet C/1973 E1 (Kohoutek) (*Herzberg and Lew,* 1974). The electronic transition is $\tilde{A}^2A_1$–$\tilde{X}^2B_1$ and it is observed from 4000 to 7500 Å; a small part of this range is seen in Fig. 7. *Wegmann et al.* (1999) have run magnetohydrodynamic and chemical simulations of cometary comae and have concluded that for small comets, up to 11% of the water molecules are ultimately ionized. H_2O^+ occurs in a spectral bandpass that is easily accessible to CCD detectors, so there are many observations of H_2O^+ in cometary comae. *Lutz et al.* (1993) have calculated fluorescence efficiency factors for six of the bands. H_2O^+ is isoelectronic to NH_2 so *Arpigny*'s (1994) comment concerning increasing the efficiency factors of NH_2 by a factor of 2 also applies to H_2O^+. Indeed, although the standard reference on the H_2O^+ band (*Lew,* 1976) used the linear notation, the transitions are more correctly specified in their bent notation (*Cochran and Cochran,* 2002).

Bonev and Jockers (1994) mapped the distribution of H_2O^+ in Comet C/1989 X1 (Austin). They found a strong asymmetry with a relatively flat distribution tailward and a

factor of 4 dropoff in the first 10^4 km sunward. The maximum H_2O^+ column density was frequently observed to be shifted tailward.

CO_2^+ emission was first identified in the optical spectrum of Comet C/1947 S1 (Bester) (*Swings and Page,* 1950) and in the UV spectrum of Comet C/1975 V1 (West) (*Feldman and Brune,* 1976). The optical lines arise from the Fox-Duffendack-Barker ($\tilde{A}^2\Pi_u$–$\tilde{X}^2\Pi_g$) electronic band system and appear in the wavelength range from 3000 to 4000 Å. The UV doublet at 2890 Å is from the $\tilde{B}^2\Sigma_u$–$\tilde{X}^2\Pi_g$ electronic transition (*Festou et al.,* 1982). *Feldman et al.* (1986), using the IUE, noted a strong enhancement of this feature in a spectrum of Comet 1P/Halley taken at a position 150,000 km tailward of the nucleus at a time corresponding to the peak of an optical outburst. This observation suggested that CO_2 may have played a significant role in the outburst process.

Leach (1987) has noted that the CO_2^+ emission rates are affected by intramolecular coupling between the $\tilde{B}^2\Sigma_u$ and $\tilde{A}^2\Pi_u$ states so that emission from the $\tilde{B}^2\Sigma_u$ state can occur at $\lambda > 3000$ Å (this is referred to as "redshifted fluorescence"). Such bands are detected in cometary spectra along with some unclassified bands redward of 4000 Å. Excitation efficiencies for some of the transitions can be found in *Fox and Dalgarno* (1979).

Bands of the OH^+ $A^3\Pi$–$X^3\Sigma^-$ electronic system cover the complete optical bandpass. However, only lines from the (0,0) and (1,0) bands have been detected (*Swings and Page,* 1950; *Festou et al.,* 1982). *Lutz et al.* (1993) have derived fluorescence efficiency factors for many bands of OH^+, but caution that they are only accurate to ±50% because the Swings effect was not included.

The CH^+ lines that are seen in cometary spectra are from a $A^1\Pi$–$X^1\Sigma$ transition. Only the low-energy transitions of the (0,0) band are seen at around 4230 Å. These lines are coincident with bands of CH and CO^+. *Lutz et al.* (1993) have also calculated g-factors for CH^+. As with the OH^+, they caution that the Swings effect was not included and therefore the fluorescence efficiencies are only good to ±50%.

Other molecular ions were detected by the *in situ* mass spectrometer measurements made at Comet Halley in 1986. These include H_3S^+, C_3H^+, and $C_3H_3^+$, as well as more complex organic ions (*Marconi et al.,* 1990; *Eberhardt and Krankowsky,* 1995). Attempts to associate some of the unidentified visible spectral features with ions such as these or with H_2S^+ must be taken with caution.

8.2. The Case of N_2^+

N_2 is the least reactive of all N-bearing species, so study of N_2 is important for understanding cometary N. In addition, conditions in the early solar nebula were such that the dominant equilibrium species of N should be N_2. However, observations of N_2 are extremely difficult to obtain. Ground-based observations suffer from telluric absorption; interpretations of spacecraft flyby mass spectrometer data are compromised by the fact that N_2 and CO both share the mass 28 bin. Therefore, observations of the First Negative ($B^2\Sigma_u^+$–$X^1\Sigma_g^+$) (0,0) band of N_2^+ at 3914 Å have been used as a proxy for studying N_2. Such observations require high spectral resolution in order to isolate the cometary N_2^+ emission from any telluric N_2^+ emission. They also require a relatively bright comet with a well-developed ion tail for observation. The spatial distribution of any emissions can be used to differentiate between telluric and cometary species.

Observations of the appropriate spectral region of the tails of comets have been made in the past, and examples of comets that show N_2^+ in their spectra can be found in *Swings and Haser* (1956) (e.g., Comet Bester, plate XXIIIa, and Comet Morehouse, plates VIa and VIb). *Cochran et al.* (2000) summarized most of the past N_2^+ observations. These observations have *not* generally been obtained at high spectral resolving power. Recently, Cochran and co-workers (*Cochran et al.,* 2000; *Cochran,* 2002) have reported high-spectral-resolution, high-signal-to-noise observations of three comets that definitely do *not* show N_2^+ in their spectra and that have very tight limits on the quantity of N_2^+. Do different comets have differing amounts of N_2, possibly related to their place of origin? Is N_2 depleted during the life of some comets? Are our models that indicate that N should be preferentially in N_2 rather than NH_3 in the solar nebula in error? Are variations in the quantity of N_2 in comets the result of clathration of the N_2 and CO (*Iro et al.,* 2003)? And ultimately, how reliable are the earlier reports of N_2^+ in cometary tail spectra? Answers to these important questions will require more high-spectral-resolution observations of comets with a variety of dynamical histories.

8.3. Atomic Ions

Table 2 also lists the wavelengths of the resonance transitions of the principal atomic ions. The C II doublet at 1335 Å has been detected in several comets, particularly from sounding rocket observations made with fairly large fields of view (*Feldman and Brune,* 1976; *Woods et al.,* 1987; *McPhate et al.,* 1999). It is difficult to identify the source of the emission. Resonance scattering of the solar C II lines would show a very strong Swings effect. Photoionization of neutral C into an excited ion state has an excitation rate $\sim 10^{-9}$ s^{-1} $atom^{-1}$ (*Hofmann et al.,* 1983) and is insufficient to account for the observed brightness. Perhaps electron impact ionization is responsible as the C II emission is present in the same spectra as the O I] λ1356 emission, but the excitation rate is difficult to evaluate quantitatively. C II λ1037 emission has recently been detected in FUSE spectra (*Weaver et al.,* 2002).

The only other reported atomic ion emission is O II λ834 from a rocket observation of Comet Hale-Bopp by *Stern et al.* (2000). No quantitative information about this measurement is given.

Despite the large number of spectra covering this wavelength range from IUE and HST, the S II triplet at 1256 Å has never been detected.

9. OUTLOOK

The study of the gaseous content of cometary comae has seen much progress during the past two decades due to both enhancements in technology, enabling many more species to be observed, and to a better understanding of the physical processes producing the observed emissions. Spectroscopy continues to be a powerful tool that remains ahead of the laboratory data needed to identify the still large number of unexplained features seen in high-resolution spectra both in the visible (*Cochran and Cochran,* 2002) and the far-UV (*Weaver et al.,* 2002). The large database of observations, dating back more than a century, provides an important tool to assess the chemical and evolutionary diversity of comets.

Acknowledgments. P.D.F. wishes to thank the Institut d'Astrophysique de Paris for their hospitality while he held a Poste Rouge from the CNRS during the fall of 2002. This work was partially supported by NASA grants NAG5-9003 (A.L.C.), NAG5-8942 (M.R.C.), and NAG5-5315 (P.D.F.).

REFERENCES

A'Hearn M. F. (1982) Spectrophotometry of comets at optical wavelengths. In *Comets* (L. L. Wilkening, ed.), pp. 433–460. Univ. of Arizona, Tucson.

A'Hearn M. F. and Feldman P. D. (1980) Carbon in Comet Bradfield 1979l. *Astrophys. J. Lett., 242,* L187–L190.

A'Hearn M. F. and Schleicher D. G. (1988) Comet P/Encke's nongravitational force. *Astrophys. J. Lett., 331,* L47–L51.

A'Hearn M. F., Schleicher D. G., and West R. A. (1985) Emission by OD in comets. *Astrophys. J., 297,* 826–836.

A'Hearn M. F., Millis R. L., Schleicher D. G., Osip D. J., and Birch P. V. (1995) The ensemble properties of comets: Results from narrowband photometry of 85 comets, 1976–1992. *Icarus, 118,* 223–270.

A'Hearn M. F., Wellnitz D. D., Woodney L., Feldman P. D., Weaver H. A., Arpigny C., Meier R., Jackson W. M., and Kim S. J. (1999) S_2 in Comet Hyakutake. *Bull. Am. Astron. Soc., 31,* 1124.

Arpigny C. (1965) Spectra of comets and their interpretation. *Annu. Rev. Astron. Astrophys., 3,* 351–375.

Arpigny C. (1994) Physical chemistry of comets: Models, uncertainties, data needs. In *Molecules and Grains in Space* (I. Nenner, ed.), pp. 205–238. AIP Conference Proceedings 312.

Arpigny C., Magain P., Manfroid J., Dossin F., Danks A. C., and Lambert K. L. (1987) Resolution of the [O I] + NH_2 blend in Comet P/Halley. *Astron. Astrophys., 187,* 485–488.

Arpigny C., Rauer H., Manfroid J., Hutsemékers D., Jehin E., Crovisier J., and Jorda L. (1998) Production and kinematics of sodium atoms in the coma of comet Hale-Bopp. *Astron. Astrophys., 334,* L53–L56.

Arpigny C., Jehin E., Manfroid J., Hutsemékers D., Schulz R., Stüwe J. A., Zucconi J.-M., and Ilyin I. (2003) Anomalous nitrogen isotope ratio in comets. *Science, 301,* 1522–1524.

Azoulay G. and Festou M. C. (1986) The abundance of sulphur in comets. In *Asteroids, Comets, Meteors II,* pp. 273–277.

Bappu M. K. V. and Sivaraman K. R. (1969) Some characteristics of the solar wind inferred from the study of sodium emission from cometary nuclei. *Sol. Phys., 10,* 496–501.

Bar-Nun A. and Prialnik D. (1988) The possible formation of a hydrogen coma around comets at large heliocentric distances. *Astrophys. J. Lett., 324,* L31–L34.

Bertaux J. L. (1986) The UV bright spot of water vapor in comets. *Astron. Astrophys., 160,* L7–L10.

Bertaux J. L., Blamont J. E., and Festou M. (1973) Interpretation of hydrogen Lyman-alpha observations of Comets Bennett and Encke. *Astron. Astrophys., 25,* 415–430.

Bird M. K., Huchtmeier W. K., Gensheimer P., Wilson T. L., Janardhan P., and Lemme C. (1997) Radio detection of ammonia in comet Hale-Bopp. *Astron. Astrophys., 325,* L5–L8.

Biver N., Bockelée-Morvan D., Colom P., Crovisier J., Germain B., Lellouch E., Davies J. K., Dent W. R. F., Moreno R., Paubert G., Wink J., Despois D., Lis D. C., Mehringer D., Benford D., Gardner M., Phillips T. G., Gunnarsson M., Rickman H., Winnberg A., Bergman P., Johansson L. E. B., and Rauer H. (1999) Long-term evolution of the outgassing of Comet Hale-Bopp from radio observations. *Earth Moon Planets, 78,* 5–11.

Bockelée-Morvan D. and Crovisier J. (1985) Possible parents for the cometary CN radical — Photochemistry and excitation conditions. *Astron. Astrophys., 151,* 90–100.

Bockelée-Morvan D. and Gérard E. (1984) Radio observations of the hydroxyl radical in comets with high spectral resolution — Kinematics and asymmetries of the OH coma in C/Meier (1978 XXI), C/Bradfield (1979X), and C/Austin (1982g). *Astron. Astrophys., 131,* 111–122.

Bockelée-Morvan D., Crovisier J., and Gérard E. (1990) Retrieving the coma gas expansion velocity in P/Halley, Wilson (1987 VII) and several other comets from the 18-cm OH line shapes. *Astron. Astrophys., 238,* 382–400.

Bockelée-Morvan, D., Lis D. C., Wink J. E., Despois D., Crovisier J., Bachiller R., Benford D. J., Biver N., Colom P., Davies J. K., Gérard E., Germain B., Houde M., Mehringer D., Moreno R., Paubert G., Phillips T. G., and Rauer H. (2000) New molecules found in comet C/1995 O1 (Hale-Bopp). Investigating the link between cometary and interstellar material. *Astron. Astrophys., 353,* 1101–1114.

Bockelée-Morvan D., Crovisier J., Mumma M. J., and Weaver H. A. (2004) The composition of cometary volatiles. In *Comets II* (M. C. Festou et al., eds.), this volume. Univ. of Arizona, Tucson.

Bonev B. and Komitov B. (2000) New two-variable fits for the scale lengths of CN and its parent molecule in cometary atmospheres: Application to the identification of the CN parent. *Bull. Am. Astron. Soc., 32,* 1072.

Bonev T. and Jockers K. (1994) H_2O^+ ions in the inner plasma tail of Comet Austin 1990 V. *Icarus, 107,* 335–357.

Bowen I. S. (1947) Excitation by line coincidence. *Publ. Astron. Soc. Pac., 59,* 196.

Brooke T. Y., Tokunaga A. T., Weaver H. A., Crovisier J., Bockelée-Morvan D., and Crisp D. (1996) Detection of acetylene in the infrared spectrum of Comet Hyakutake. *Nature, 383,* 606–608.

Brown M. E. and Spinrad H. (1993) The velocity distribution of cometary hydrogen — Evidence for high velocities? *Icarus, 104,* 197–205.

Brown M. E., Bouchez A. H., Spinrad H., and Misch A. (1998) Sodium velocities and sources in Hale-Bopp. *Icarus, 134,* 228–234.

Brown R. A. and Chaffee F. H. (1974) High-resolution spectra of

sodium emission from Io. *Astrophys. J. Lett., 187,* L125–L126.
Budzien S. A. and Feldman P. D. (1991) OH prompt emission in Comet IRAS-Araki-Alcock (1983 VII). *Icarus, 90,* 308–318.
Budzien S. A., Festou M. C., and Feldman P. D. (1994) Solar flux variability and the lifetimes of cometary H_2O and OH. *Icarus, 107,* 164–188.
Bus S. J., A'Hearn M. F., Schleicher D. G., and Bowell E. (1991) Detection of CN emission from (2060) Chiron. *Science, 251,* 774–777.
Chamberlain J. W. and Hunten D. M. (1987) *Theory of Planetary Atmospheres: An Introduction to Their Physics and Chemistry, 2nd edition*. Academic, Orlando.
Cochran A. L. (2002) A search for N_2^+ in spectra of Comet C/2002 C1 (Ikeya-Zhang). *Astrophys. J. Lett., 576,* L165–L168.
Cochran A. L. and Cochran W. D. (1991) The first detection of CN and the distribution of CO^+ gas in the coma of Comet P/Schwassmann-Wachmann 1. *Icarus, 90,* 172–175.
Cochran A. L. and Cochran W. D. (2001) Observations of O (^{1}S) and O (^{1}D) in spectra of C/1999 S4 (LINEAR). *Icarus, 154,* 381–390.
Cochran A. L. and Cochran W. D. (2002) A high spectral resolution atlas of Comet 122P/de Vico. *Icarus, 157,* 297–308.
Cochran A. L., Cochran W. D., and Barker E. S. (2000) N_2^+ and CO^+ in Comets 122P/1995 S1 (deVico) and C/1995 O1 (Hale-Bopp). *Icarus, 146,* 583–593.
Cochran W. D. (1984) Detection of forbidden O I ^{1}S–^{1}D in comet IRAS-Araki-Alcock. *Icarus, 58,* 440–445.
Code A. D., Houck T. E., and Lillie C. F. (1972) Ultraviolet observations of comets. In *Scientific Results from the Orbiting Astronomical Observatory (OAO-2)* (A. D. Code, ed.), pp. 109–114. NASA SP-310.
Combi M. R. and Feldman P. D. (1992) IUE observations of H Lyman-alpha in Comet P/Giacobini-Zinner. *Icarus, 97,* 260–268.
Combi M. R. and Feldman P. D. (1993) Water production rates in Comet P/Halley from IUE observations of H I Lyman-alpha. *Icarus, 105,* 557–567.
Combi M. R. and Fink U. (1997) A critical study of molecular photodissociation and CHON grain sources for cometary C_2. *Astrophys. J., 484,* 879–890.
Combi M. R. and McCrosky R. E. (1991) High-resolution spectra of the 6300 Å region of Comet P/Halley. *Icarus, 91,* 270–279.
Combi M. R., DiSanti M. A., and Fink U. (1997) The spatial distribution of gaseous atomic sodium in the comae of comets: Evidence for direct nucleus and extended plasma sources. *Icarus, 130,* 336–354.
Combi M. R., Brown M. E., Feldman P. D., Keller H. U., Meier R. R., and Smyth W. H. (1998) Hubble Space Telescope ultraviolet imaging and high-resolution spectroscopy of water photodissociation products in Comet Hyakutake (C/1996 B2). *Astrophys. J., 494,* 816–821.
Combi M. R., Cochran A. L., Cochran W. D., Lambert D. L., and Johns-Krull C. M. (1999) Observation and analysis of high-resolution optical line profiles in Comet Hyakutake (C/1996 B2). *Astrophys. J., 512,* 961–968.
Combi M. R., Harris W. R., and Smyth W. M. (2004) Gas dynamics and kinetics in the cometary coma: Theory and observations. In *Comets II* (M. C. Festou et al., eds.), this volume. Univ. of Arizona, Tucson.
Cravens T. E. and Green A. E. S. (1978) Airglow from the inner comas of comets. *Icarus, 33,* 612–623.
Cravens T. E., Kozyra J. U., Nagy A. F., Gombosi T. I., and Kurtz M. (1987) Electron impact ionization in the vicinity of comets. *J. Geophys. Res., 92,* 7341–7353.
Cremonese G., Boehnhardt H., Crovisier J., Rauer H., Fitzsimmons A., Fulle M., Licandro J., Pollacco D., Tozzi G. P., and West R. M. (1997) Neutral sodium from Comet Hale-Bopp: A third type of tail. *Astrophys. J. Lett., 490,* L199–L202.
Crovisier J., Colom P., Gérard E., Bockelée-Morvan D., and Bourgois G. (2002) Observations at Nançay of the OH 18-cm lines in comets. The data base. Observations made from 1982 to 1999. *Astron. Astrophys., 393,* 1053–1064.
Delsemme A. H. and Combi M. R. (1983) Neutral cometary atmospheres. IV — Brightness profiles in the inner coma of comet Kohoutek 1973 XII. *Astrophys. J., 271,* 388–397.
Despois D., Gérard E., Crovisier J., and Kazes I. (1981) The OH radical in comets — Observation and analysis of the hyperfine microwave transitions at 1667 MHz and 1665 MHz. *Astron. Astrophys., 99,* 320–340.
Douglas A. E. (1951) Laboratory studies of the λ 4050 group of cometary spectra. *Astrophys. J., 114,* 466–468.
Durrance S. T. (1981) The carbon monoxide fourth positive bands in the Venus dayglow. I — Synthetic spectra. *J. Geophys. Res., 86,* 9115–9124.
Eberhardt P. and Krankowsky D. (1995) The electron temperature in the inner coma of comet P/Halley. *Astron. Astrophys., 295,* 795–806.
Feldman P. D. (1982) Ultraviolet spectroscopy of comae. In *Comets* (L. L. Wilkening, ed.), pp. 461–479. Univ. of Arizona, Tucson.
Feldman P. D. (1996) Comets. In *Atomic, Molecular, and Optical Physics Reference Book* (G. W. F. Drake, ed.), pp. 930–939. American Institute of Physics, New York.
Feldman P. D. and Brune W. H. (1976) Carbon production in comet West 1975n. *Astrophys. J. Lett., 209,* L45–L48.
Feldman P. D., Takacs P. Z., Fastie W. G., and Donn B. (1974) Rocket ultraviolet spectrophotometry of Comet Kohoutek (1973f). *Science, 185,* 705–707.
Feldman P. D., Opal C. B., Meier R. R., and Nicolas K. R. (1976) Far ultraviolet excitation processes in comets. In *The Study of Comets,* pp. 773–796. IAU Colloquium No. 25.
Feldman P. D., Weaver H. A., A'Hearn M. F., Festou M. C., and McFadden L. A. (1986) Is CO_2 responsible for the outbursts of comet Halley? *Nature, 324,* 433–436.
Feldman P. D., Fournier K. B., Grinin V. P., and Zvereva A. M. (1993) The abundance of ammonia in Comet P/Halley derived from ultraviolet spectrophotometry of NH by ASTRON and IUE. *Astrophys. J., 404,* 348–355.
Feldman P. D., Festou M. C., Tozzi G. P., and Weaver H. A. (1997) The CO_2/CO abundance ratio in 1P/Halley and several other comets observed by IUE and HST. *Astrophys. J., 475,* 829–834.
Feldman P. D., Weaver H. A., A'Hearn M. F., Festou M. C., McPhate J. B., and Tozzi G.-P. (1999) Ultraviolet imaging spectroscopy of Comet Lee (C/1999 H1) with HST/STIS. *Bull. Am. Astron. Soc., 31,* 1127.
Feldman P. D., Weaver H. A., and Burgh E. B. (2002) Far Ultraviolet Spectroscopic Explorer observations of CO and H_2 emission in Comet C/2001 A2 (LINEAR). *Astrophys. J. Lett., 576,* L91–L94.
Festou M. C. (1984) Aeronomical processes in cometary atmospheres — The carbon compounds' puzzle. *Adv. Space Res., 4,* 165–175.
Festou M. and Feldman P. D. (1981) The forbidden oxygen lines in comets. *Astron. Astrophys., 103,* 154–159.

Festou M. C. and Feldman P. D. (1987) Comets. In *Exploring the Universe with the IUE Satellite* (Y. Kondo et al., eds.), pp. 101–118. ASSL Vol. 129, Kluwer, Dordrecht.

Festou M., Jenkins E. B., Barker E. S., Upson W. L., Drake J. F., Keller H. U., and Bertaux J. L. (1979) Lyman-alpha observations of comet Kobayashi-Berger-Milon (1975 IX) with Copernicus. *Astrophys. J., 232,* 318–328.

Festou M. C., Feldman P. D., and Weaver H. A. (1982) The ultraviolet bands of the CO_2^+ ion in comets. *Astrophys. J., 256,* 331–338.

Festou M. C., Barale O., Davidge T., Stern S. A., Tozzi G. P., Womack M., and Zucconi J. M. (1998) Tentative identification of the parent of CN radicals in comets: = C_2N_2. *Bull. Am. Astron. Soc., 30,* 1089.

Fink U. and Hicks M. D. (1996) A survey of 39 comets using CCD spectroscopy. *Astrophys. J., 459,* 729–743.

Fink U., Combi M. R., and DiSanti M. A. (1991) Comet P/Halley — Spatial distributions and scale lengths for C_2, CN, NH_2, and H_2O. *Astrophys. J., 383,* 356–371.

Fox J. L. and Dalgarno A. (1979) Ionization, luminosity, and heating of the upper atmosphere of Mars. *J. Geophys. Res., 84,* 7315–7333.

Gérard E. (1990) The discrepancy between OH production rates deduced from radio and ultraviolet observations of comets. I — A comparative study of OH radio and UV observations of P/Halley 1986 III in late November and early December 1985. *Astron. Astrophys., 230,* 489–503.

Greenstein J. L. (1958) High-resolution spectra of Comet Mrkos (1957d). *Astrophys. J., 128,* 106–106.

Haser L. and Swings P. (1957) Sur la possibilité d'une fluorescence cométaire excitée par la raie d'émission Lyman α solaire. *Annal. Astrophys., 20,* 52.

Herzberg G. and Lew H. (1974) Tentative identification of the H_2O^+ ion in Comet Kohoutek. *Astron. Astrophys., 31,* 123–124.

Hofmann H., Saha H. P., and Trefftz E. (1983) Excitation of C II lines by photoionization of neutral carbon. *Astron. Astrophys., 126,* 415–426.

Huebner W. F. (1970) Dust from cometary nuclei. *Astron. Astrophys., 5,* 286–297.

Huebner W. F., Keady J. J., and Lyon S. P., eds. (1992) *Solar Photo Rates for Planetary Atmospheres and Atmospheric Pollutants*. Kluwer, Dordrecht. 292 pp.

Huppler D., Reynolds R. J., Roesler F. L., Scherb F., and Trauger J. (1975) Observations of comet Kohoutek (1973f) with a ground-based Fabry-Perot spectrometer. *Astrophys. J., 202,* 276–282.

Iro N., Gautier D., Hersant F., Bockelée-Morvan D., and Lunine J. I. (2003) An interpretation of the nitrogen deficiency in comets. *Icarus, 161,* 511–532.

Irvine W. M., Senay M., Lovell A. J., Matthews H. E., McGonagle D., and Meier R. (2000) Detection of nitrogen sulfide in Comet Hale-Bopp. *Icarus, 143,* 412–414.

Jackson W. M. (1976) The photochemical formation of cometary radicals. *J. Photochem., 5,* 107–118.

Jackson W. M. and Donn B. (1968) Photochemical effects in the production of cometary radicals and ions. *Icarus, 8,* 270–280.

Jackson W. M., Halpern J. B., Feldman P. D., and Rahe J. (1982) Production of CS and S in Comet Bradfield (1979 X). *Astron. Astrophys., 107,* 385–389.

Jackson W. M., Butterworth P. S., and Ballard D. (1986) The origin of CS in comet IRAS-Araki-Alcock 1983d. *Astrophys. J., 304,* 515–518.

Jessberger E. K. and Kissel J. (1991) Chemical properties of cometary dust and a note on carbon isotopes. In *Comets in the Post-Halley Era* (R. Newburn et al., eds.), pp. 1075–1092. IAU Colloquium No. 116, ASSL Vol. 167, Kluwer, Dordrecht.

Kawakita H., Watanabe J., Ando H., Aoki W., Fuse T., Honda S., Izumiura H., Kajino T., Kambe E., Kawanomoto S., Noguchi K., Okita K., Sadakane K., Sato B., Takada-Hidai M., Takeda Y., Usuda T., Watanabe E., and Yoshida M. (2001a) The spin temperature of NH_3 in Comet C/1999S4 (LINEAR). *Science, 294,* 1089–1091.

Kawakita H., Watanabe J., Kinoshita D., Abe S., Furusyo R., Izumiura H., Yanagisawa K., and Masuda S. (2001b) High-dispersion spectra of NH_2 in the Comet C/1999 S4 (LINEAR): Excitation mechanism of the NH_2 molecule. *Publ. Astron. Soc. Japan, 53,* L5–L8.

Keller H. U. (1976) The interpretations of ultraviolet observations of comets. *Space Sci. Rev., 18,* 641–684.

Kim S. J. and A'Hearn M. F. (1991) Upper limits of SO and SO_2 in comets. *Icarus, 90,* 79–95.

Kim S. J. and A'Hearn M. F. (1992) G-factors of the SH (0-0) band and SH upper limit in Comet P/Brorsen-Metcalf (1989o). *Icarus, 97,* 303–306.

Kim S. J., A'Hearn M. F., and Cochran W. D. (1989) NH emissions in comets — Fluorescence vs. collisions. *Icarus, 77,* 98–108.

Kleine M., Wyckoff S., Wehinger P. A., and Peterson B. A. (1994) The cometary flourescence spectrum of cyanogen: A model. *Astrophys. J., 436,* 885–906.

Kleine M., Wyckoff S., Wehinger P. A., and Peterson B. A. (1995) The carbon isotope abundance ratio in comet Halley. *Astrophys. J., 439,* 1021–1033.

Korsun P. P. and Jockers K. (2002) CN, NH_2, and dust in the atmosphere of comet C/1999 J3 (LINEAR). *Astron. Astrophys., 381,* 703–708.

Krasnopolsky V. A. and Tkachuk A. Y. (1991) TKS-Vega experiment — NH and NH_2 bands in Comet Halley. *Astrophys. J., 101,* 1915–1919.

Krishna Swamy K. S. (1997) On the rotational population distribution of C_2 in comets. *Astrophys. J., 481,* 1004–1006.

Krishna Swamy K. S. and Tarafdar S. P. (1993) Study of the A-X (0,0) band profile of CS in comets. *Astron. Astrophys., 271,* 326–334.

Lambert D. L. and Danks A. C. (1983) High-resolution spectra of C_2 Swan bands from comet West 1976 VI. *Astrophys. J., 268,* 428–446.

Lambert D. L., Sheffer Y., Danks A. C., Arpigny C., and Magain P. (1990) High-resolution spectroscopy of the C_2 Swan 0-0 band from Comet P/Halley. *Astrophys. J., 353,* 640–653.

Leach S. (1987) Electronic spectroscopy and relaxation of some molecular cations of cometary interest. *Astron. Astrophys., 187,* 195–200.

Lean J. (1991) Variations in the sun's radiative output. *Rev. Geophys., 29,* 505–535.

Levin B. J. (1964) On the reported Na tails of comets. *Icarus, 3,* 497–498.

Lew H. (1976) Electronic spectrum of H_2O^+. *Can. J. Phys., 54,* 2028–2049.

Lis D. C., Mehringer D. M., Benford D., Gardner M., Phillips T. G., Bockelée-Morvan D., Biver N., Colom P., Crovisier J., Despois D., and Rauer H. (1999) New molecular species in Comet C/1995 O1 (Hale-Bopp) observed with the Caltech Submillimeter Observatory. *Earth Moon Planets, 78,* 13–20.

Lutz B. L., Womack M., and Wagner R. M. (1993) Ion abundances and implications for photochemistry in Comets Halley (1986 III) and Bradfield (1987 XXIX). *Astrophys. J., 407,* 402–411.

Magee-Sauer K., Roesler F. L., Scherb F., Harlander J., and Oliversen R. J. (1988) Spatial distribution of O(^{1}D) from Comet Halley. *Icarus, 76,* 89–99.

Magee-Sauer K., Dello Russo N., DiSanti M. A., Gibb E., and Mumma M. J. (2002) CSHELL observations of Comet C/2002 C1 (Ikeya-Zhang) in the 3.0-micron region. *Bull. Am. Astron. Soc., 34,* 868.

Magnani L. and A'Hearn M. F. (1986) CO^+ fluorescence in comets. *Astrophys. J., 302,* 477–487.

Marconi M. L., Mendis D. A., Korth A., Lin R. P., Mitchell D. L., and Reme H. (1990) The identification of H_3S^+ with the ion of mass per charge (m/q) 35 observed in the coma of Comet Halley. *Astrophys. J. Lett., 352,* L17–L20.

McPhate J. B., Feldman P. D., McCandliss S. R., and Burgh E. B. (1999) Rocket-borne long-slit ultraviolet spectroscopy of Comet Hale-Bopp. *Astrophys. J., 521,* 920–927.

Meier R. and A'Hearn M. F. (1997) Atomic sulfur in cometary comae based on UV spectra of the S I triplet near 1814 Å. *Icarus, 125,* 164–194.

Morrison N. D., Knauth D. C., Mulliss C. L., and Lee W. (1997) High-resolution optical spectra of the head of the Comet C/1996 B2 (Hyakutake). *Publ. Astron. Soc. Pac., 109,* 676–681.

Mumma M. J., Stone E. J., and Zipf E. C. (1975) Nonthermal rotational distribution of CO ($A^1\Pi$) fragments produced by dissociative excitation of CO_2 by electron impact. *J. Geophys. Res., 80,* 161–167.

Mumma M. J., McLean I. S., DiSanti M. A., Larkin J. E., Russo N. D., Magee-Sauer K., Becklin E. E., Bida T., Chaffee F., Conrad A. R., Figer D. F., Gilbert A. M., Graham J. R., Levenson N. A., Novak R. E., Reuter D. C., Teplitz H. I., Wilcox M. K., and Xu L. (2001) A survey of organic volatile species in Comet C/1999 H1 (Lee) using NIRSPEC at the Keck Observatory. *Astrophys. J., 546,* 1183–1193.

Newall H. F. (1910) On the spectrum of the daylight comet 1910a. *Mon. Not. R. Astron. Soc., 70,* 459–461.

O'Dell C. R., Robinson R. R., Krishna Swamy K. S., McCarthy P. J., and Spinrad H. (1988) C_2 in Comet Halley — Evidence for its being third generation and resolution of the vibrational population discrepancy. *Astrophys. J., 334,* 476–488.

Oliversen R. J., Doane N., Scherb F., Harris W. M., and Morgenthaler J. P. (2002) Measurements of [C I] emission from Comet Hale-Bopp. *Astrophys. J., 581,* 770–775.

Opal C. B., Carruthers G. R., Prinz D. K., and Meier R. R. (1974) Comet Kohoutek: Ultraviolet images and spectrograms. *Science, 185,* 702–705.

Oppenheimer M. (1980) Sodium D-line emission in Comet West (1975n) and the sodium source in comets. *Astrophys. J., 240,* 923–928.

Palmer P., Wootten A., Butler B., Bockelée-Morvan D., Crovisier J., Despois D., and Yeomans D. K. (1996) Comet Hyakutake: First secure detection of ammonia in a comet. *Bull. Am. Astron. Soc., 28,* 927.

Pirronello V., Strazzulla G., and Foti G. (1983) H_2 production in comets. *Astron. Astrophys., 118,* 341–344.

Potter A. and Morgan T. (1985) Discovery of sodium in the atmosphere of Mercury. *Science, 229,* 651–653.

Potter A. E. and Morgan T. H. (1988) Discovery of sodium and potassium vapor in the atmosphere of the moon. *Science, 241,* 675–680.

Preston G. W. (1967) The spectrum of Ikeya-Seki (1965f). *Astrophys. J., 147,* 718–742.

Prisant M. G. and Jackson W. M. (1987) A rotational-state population analysis of the high-resolution IUE observation of CS emission in comet P/Halley. *Astron. Astrophys., 187,* 489–496.

Randall C. E., Schleicher D. G., Ballou R. G., and Osip D. J. (1992) Observational constraints on molecular scalelengths and lifetimes in comets. *Bull. Am. Astron. Soc., 24,* 1002.

Rauer H., Arpigny C., Manfroid J., Cremonese G., and Lemme C. (1998) The spatial sodium distribution in the coma of comet Hale-Bopp (C/1995 O1). *Astron. Astrophys., 334,* L61–L64.

Rauer H., Helbert J., Arpigny C., Benkhoff J., Bockelée-Morvan D., Boehnhardt H., Colas F., Crovisier J., Hainaut O., Jorda L., Kueppers M., Manfroid J., and Thomas N. (2003) Long-term optical spectrophotometric monitoring of comet Hale-Bopp (C/1995 O1). *Astron. Astrophys., 397,* 1109–1122.

Richter K., Combi M. R., Keller H. U., and Meier R. R. (2000) Multiple scattering of hydrogen Lyα radiation in the coma of Comet Hyakutake (C/1996 B2). *Astrophys. J., 531,* 599–611.

Rousselot P., Arpigny C., Rauer H., Cochran A. L., Gredel R., Cochran W. D., Manfroid J., and Fitzsimmons A. (2001) A fluorescence model of the C_3 radical in comets. *Astron. Astrophys., 368,* 689–699.

Scherb F. (1981) Hydrogen production rates from ground-based Fabry-Perot observations of comet Kohoutek. *Astrophys. J., 243,* 644–650.

Schleicher D. G. and A'Hearn M. F. (1988) The fluorescence of cometary OH. *Astrophys. J., 331,* 1058–1077.

Schleicher D. G. and Farnham T. L. (2004) Photometry and imaging of the coma with narrowband filters. In *Comets II* (M. C. Festou et al., eds.), this volume. Univ. of Arizona, Tucson.

Schleicher D. G. and Millis R. L. (1989) Revised scale lengths for cometary NH. *Astrophys. J., 339,* 1107–1114.

Singh P. D. and Dalgarno A. (1987) Photodissociation lifetimes of CH and CD radicals in comets. In *Diversity and Similarity of Comets* (E. J. Rolfe and B. Battrick, eds.), pp. 177–179. ESA SP-278, Noordwijk, The Netherlands.

Slaughter C. D. (1969) The emission spectrum of Comet Ikeya-Seki 1965f at perihelion passage. *Astrophys. J., 74,* 929–943.

Smith A. M., Stecher T. P., and Casswell L. (1980) Production of carbon, sulfur, and CS in Comet West. *Astrophys. J., 242,* 402–410.

Smith W. H. and Schempp W. V. (1989) [O I] in Comet Halley. *Icarus, 82,* 61–66.

Sorkhabi O., Blunt V. M., Lin H., A'Hearn M. F., Weaver H. A., Arpigny C., and Jackson W. M. (1997) Using photochemistry to explain the formation and observation of C_2 in comets. *Planet. Space Sci., 45,* 721–730.

Spinrad H. (1982) Observations of the red auroral oxygen lines in nine comets. *Publ. Astron. Soc. Pac., 94,* 1008–1016.

Spinrad H. and Miner E. D. (1968) Sodium velocity fields in Comet 1965f. *Astrophys. J., 153,* 355–366.

Stern S. A., Slater D. C., Festou M. C., Parker J. W., Gladstone G. R., A'Hearn M. F., and Wilkinson E. (2000) The discovery of argon in Comet C/1995 O1 (Hale-Bopp). *Astrophys. J. Lett., 544,* L169–L172.

Storey P. J. and Zeippen C. J. (2000) Theoretical values for the [O III] 5007/4959 line-intensity ratio and homologous cases. *Mon. Not. R. Astron. Soc., 312,* 813–816.

Swings P. (1941) Complex structure of cometary bands tentatively ascribed to the contour of the solar spectrum. *Lick Observatory Bull., 508,* 131–136.

Swings P. (1965) Cometary spectra (George Darwin lecture). *Quart. J. R. Astron. Soc., 6,* 28–69.

Swings P. and Haser L. (1956) *Atlas of Representative Cometary Spectra*. Impr. Ceuterick, Louvain.

Swings P. and Page T. (1950) The spectrum of Comet Bester (1947k). *Astrophys. J., 111,* 530–554.

Swings P., Elvey C. T., and Babcock H. W. (1941) The spectrum of Comet Cunningham, 1940C. *Astrophys. J., 94,* 320–343.

Tacconi-Garman L. E., Schloerb F. P., and Claussen M. J. (1990) High spectral resolution observations and kinematic modeling of the 1667 MHz hyperfine transition of OH in Comets Halley (1982i), Giacobini-Zinner (1984e), Hartley-Good (1985l), Thiele (1985m), and Wilson (1986l). *Astrophys. J., 364,* 672–686.

Tatum J. B. (1984) Cyanogen radiance/column-density ratio for comets calculated from the Swings effect. *Astron. Astrophys., 135,* 183–187.

Tatum J. B. and Gillespie M. I. (1977) The cyanogen abundance of comets. *Astrophys. J., 218,* 569–572.

Tegler S. and Wyckoff S. (1989) NH_2 fluorescence efficiencies and the NH_3 abundance in Comet Halley. *Astrophys. J., 343,* 445–449.

Tokaryk D. W. and Chomiak D. E. (1997) Laser spectroscopy of C_3: Stimulated emission and absorption spectra of the $\tilde{A}^1\Pi_u$–$\tilde{X}^1\Sigma_g^+$ transition. *J. Chem. Phys., 106,* 7600–7608.

Tozzi G. P., Feldman P. D., and Festou M. C. (1998) Origin and production of C(^{1}D) atoms in cometary comae. *Astron. Astrophys., 330,* 753–763.

Umbach R., Jockers K., and Geyer E. H. (1998) Spatial distribution of neutral and ionic constituents in comet P/Halley. *Astron. Astrophys., 127,* 479–495.

Weaver H. A. (1998) Comets. In *The Scientific Impact of the Goddard High Resolution Spectrograph* (J. C. Brandt et al., eds.), pp. 213–226. ASP Conference Series 143, Astronomical Society of the Pacific, San Francisco.

Weaver H. A., Feldman P. D., McPhate J. B., A'Hearn M. F., Arpigny C., and Smith T. E. (1994) Detection of CO Cameron band emission in comet P/Hartley 2 (1991 XV) with the Hubble Space Telescope. *Astrophys. J., 422,* 374–380.

Weaver H. A., Feldman P. D., A'Hearn M. F., Arpigny C., Brandt J. C., and Stern S. A. (1999) Post-perihelion HST observations of Comet Hale-Bopp (C/1995 O1). *Icarus, 141,* 1–12.

Weaver H. A., Feldman P. D., Combi M. R., Krasnopolsky V., Lisse C. M., and Shemansky D. E. (2002) A search for argon and O VI in three comets using the Far Ultraviolet Spectroscopic Explorer. *Astrophys. J. Lett., 576,* L95–L98.

Wegmann R., Jockers K., and Bonev T. (1999) H_2O^+ ions in comets: Models and observations. *Planet. Space Sci., 47,* 745–763.

Wilkening L. L., ed. (1982) *Comets*. Univ. of Arizona, Tucson. 766 pp.

Wilson J. K., Baumgardner J., and Mendillo M. (1998) Three tails of comet Hale-Bopp. *Geophys. Res. Lett., 25,* 225–228.

Wolven B. C. and Feldman P. D. (1998) Lyman-α induced fluorescence of H_2 and CO in comets and planetary atmospheres. In *The Scientific Impact of the Goddard High Resolution Spectrograph* (J. C. Brandt et al., eds.), pp. 373–377. ASP Conference Series 143, Astronomical Society of the Pacific, San Franciso.

Woodney L. M., A'Hearn M. F., Schleicher D. G., Farnham T. L., McMullin J. P., Wright M. C. H., Veal J. M., Snyder L. E., de Pater I., Forster J. R., Palmer P., Kuan Y.-J., Williams W. R., Cheung C. C., and Smith B. R. (2002) Morphology of HCN and CN in Comet Hale-Bopp (1995 O1). *Icarus, 157,* 193–204.

Woods T. N., Feldman P. D., and Dymond K. F. (1987) The atomic carbon distribution in the coma of Comet P/Halley. *Astron. Astrophys., 187,* 380.

Woods T. N., Feldman P. D., and Rottman G. J. (2000) Ultraviolet observations of Comet Hale-Bopp (C/1995 O1) by the UARS SOLSTICE. *Icarus, 144,* 182–186.

Wright M. C. H., de Pater I., Forster J. R., Palmer P., Snyder L. E., Veal J. M., A'Hearn M. F., Woodney L. M., Jackson W. M., Kuan Y.-J., and Lovell A. J. (1998) Mosaicked images and spectra of J = 1 → 0 HCN and HCO^+ emission from Comet Hale-Bopp (1995 O1). *Astrophys. J., 116,* 3018–3028.

Ziurys L. M., Savage C., Brewster M. A., Apponi A. J., Pesch T. C., and Wyckoff S. (1999) Cyanide chemistry in Comet Hale-Bopp (C/1995 O1). *Astrophys. J. Lett., 527,* L67–L71.